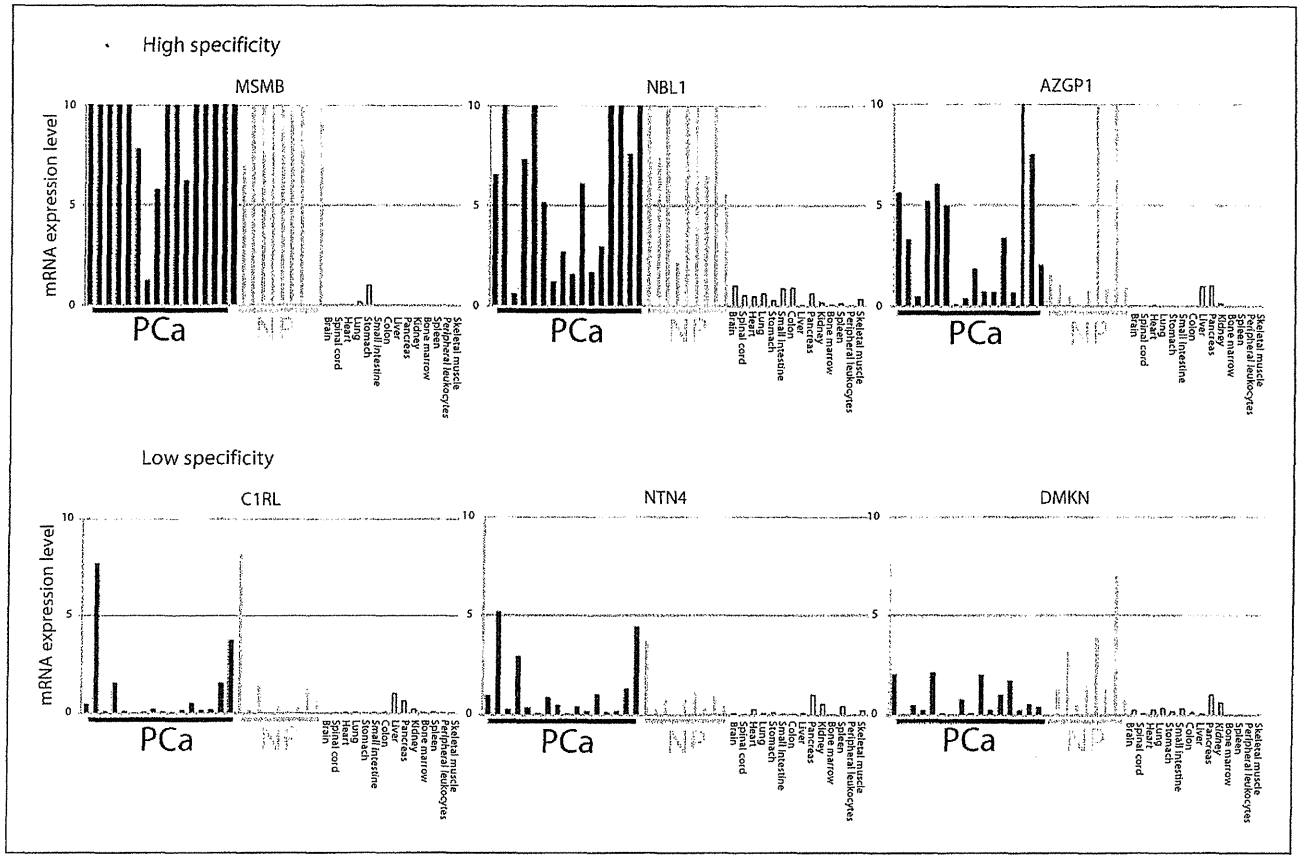

Fig. 1. Quantitative RT-PCR analysis of candidate genes in 16 PCa samples, 9 NP samples, and 14 kinds of normal tissues. MSMB, NBL1 and AZGP1 were found to show high specificity for the prostate. C1RL, NTN4 and DMKN were found to show low specificity for the prostate.

PSA is also specific for prostate and not specific for PCa, we examined these prostate-specific genes. Of the 15 candidates, 3 genes, *MSMB*, *NBL1* and *AZGP1*, were found to show high specificity for the prostate, and 3 genes, *C1RL*, *NTN4* and *DMKN*, were found to show low specificity for the prostate. Of the 3 genes showing high specificity, MSMB (microseminoprotein-β) and AZGP1 (zinc-α_2-glycoprotein) have already been studied in PCa, and their utility as serum tumor marker and therapeutic target have been reported [24–27]. Therefore, we focused on *NBL1*. *NBL1* has been reported as one of the genes whose expression is reduced in PCa compared with NP by profiling of expressed sequence tags and quantitative RT-PCR analysis [28, 29]. However, there is no report, to our knowledge, in which *NBL1* expression in human systemic organs is compared and NBL1 expression in PCa and NP determined by immunohistochemical analysis has not been reported.

We compared *NBL1* mRNA expression between prostate and systemic normal organs. The average *NBL1* mRNA expression levels in NP and PCa were 19.9- and 8.1-fold greater, respectively, than in brain, in which *NBL1* is most highly expressed of the systemic normal organs. In comparison with that in the other systemic organs, the expression of *NBL1* mRNA is highly restricted to the prostate.

NBL1 Protein Expression in Cell Lysate and Culture Medium

To study whether NBL1 is a secreted protein, we performed Western blot analysis in 3 PCa cell lines. In cell lysate, moderate NBL1 expression was detected in DU145 cells as a band of approximately 27 kDa. LNCaP cells showed low NBL1 expression, and NBL1 expression was absent in PC3 cells (fig. 2a). In culture medium, very high NBL1 expression was noted in DU145 cells, low NBL1 ex-

Table 3. Summary of quantitative RT-PCR analysis of candidate genes specifically expressed in PCa and NP samples

Gene name	Name of normal organ with highest expression	PCa with highest mRNA expression level (A)	NP with highest mRNA expression level (B)	PCa specificity index (A/B)	PCa cases with mRNA expression level ≥10-fold normal organ with highest expression	NP cases with mRNA expression level ≥10-fold normal organ with highest expression
High specificity						
MSMB	Stomach	>100	>100	0.13	12	8
NBL1	Brain	29.6	71.2	0.42	5	5
AZGP1	Pancreas	21.5	22.4	0.96	1	2
Low specificity						
C1RL	Liver	7.7	8.2	0.94	0	0
NTN4	Pancreas	5.2	3.7	1.4	0	0
DMKN	Pancreas	2.1	7.0	0.3	0	0
No specificity						
FN1	Liver	0.78	0.37	2.1	0	0
COL4A5	Stomach	0.72	0.69	1.0	0	0
CCDC126	Skeletal muscle	0.58	0.07	8.3	0	0
SPP1	Kidney	0.56	0.34	1.6	0	0
CALU	Heart	0.32	0.26	1.2	0	0
CLU	Liver	0.3	1.0	0.3	0	0
SRGN	Bone marrow	0.27	0.67	0.4	0	0
FGB	Liver	<0.01	<0.01	–	0	0
TFPI	Kidney	<0.01	0.022	–	0	0
SFTPA1B	Lung	0.057	<0.01	–	0	0
ARMETL	Skeletal muscle	<0.01	<0.01	–	0	0

Target mRNA expression levels were standardized to 1.0 μg total RNA from the normal organ with the highest expression set as 1.0 (16 PCa and 9 NP samples).

pression was seen in LNCaP cells, and no expression of NBL1 was noted in PC3 cells. In the CAST analysis, colonies containing the *NBL1* gene were detected in the DU145 CAST library, indicating that Western blot analysis of NBL1 protein was consistent with CAST analysis. Next, we examined transition of NBL1 expression by Western blot analysis of cell extracts of DU145 transfected with *NBL1*-specific siRNAs. Two types of siRNAs (siRNA1 and siRNA2) and negative control siRNA were transfected into DU145 cell extracts. Expression of NBL1 in DU145 was suppressed by treatment with siRNA1 and siRNA2 in both cell lysate and culture medium (fig. 2b).

Immunohistochemical Analysis of NBL1 Expression in Normal Systemic Organs

We performed immunohistochemical analysis of NBL1 in 19 kinds of non-cancerous systemic tissues in 5 samples of each tissue. NBL1 expression was detected only in epithelium of the small intestine and colon, islets of the pancreas, and nerve cells in brain and spinal cord (fig. 3a–d). We did not detect the expression of NBL1 in heart, lung, esophagus, stomach, liver, spleen, pancreas, kidney, adrenal, ureter, bladder, testis, skin, skeletal muscle and vessel. When the level of NBL1 expression is compared in small intestine and colon, islets of the pancreas, and nerve cells in brain and spinal cord, expression in the brain nerve cells is higher than in the other tissues. These results are consistent with our quantitative RT-PCR results.

Immunohistochemical Analysis of NBL1 Expression in PCa and NP

We also performed immunohistochemical analysis of NBL1 in a total of 194 prostate samples, which included BPH in 13 patients and PCa in 181 patients. The clinical characteristics of the PCa patients are summarized in table 1. NBL1 staining was observed in the cytoplasm of both NP epithelium and cancer cells. In some acini, NBL1 expression was stronger at the apical side of luminal cells

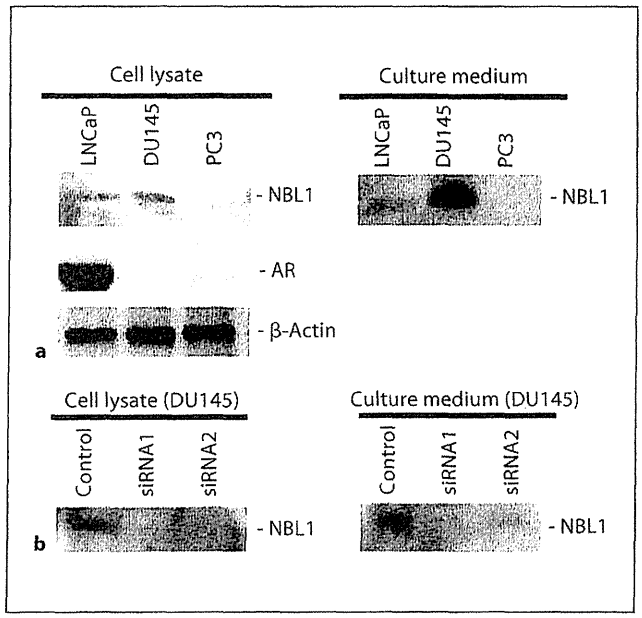

Fig. 2. Western blot analysis of NBL1 protein in PCa cell lines. NBL1 expression in DU145 and LNCaP cell lines was observed in cell lysate. In culture medium, high NBL1 expression was noted in DU145 cells (**a**). NBL1 expression in DU145 was suppressed by treatment with siRNA1 and siRNA2 in both cell lysate and culture medium (**b**).

and was detected in the prostatic ducts. Expression of NBL1 was not detected in stromal cells. Although NBL1 expression in PCa cells has some heterogeneity, NBL1 expression was detected in 1–95% of all samples (fig. 3e–h). All prostate samples were considered NBL1 positive if any cell stained positive. These immunohistochemical results suggest that NBL1 was highly expressed in and restricted to the prostate.

Next, we compared clinicopathological parameters with NBL1 expression scores in the prostate samples (fig. 4a–d). Mean NBL1 expression score was significantly higher in BPH samples and NP adjacent to PCa than in PCa itself ($p < 0.0001$). The mean NBL1 expression score was significantly higher in PCa classified as stage B than in PCa classified as stages C and D ($p = 0.0014$) and was significantly higher in PCa with Gleason score 6 than in PCa with Gleason score 7–10 ($p = 0.0024$). The mean NBL1 expression score was also significantly higher in PCa with PSA level ≤20 than in PCa with PSA level >20 ($p < 0.0001$).

Effect of NBL1 Inhibition on Cell Growth and Invasive Activity of PCa Cells

We studied the biological role of NBL1 using the DU145 cell line because of the high expression of NBL1 in this cell line. To investigate the possible proliferative effects of NBL1 knockdown, we performed an MTT assay 4 days after siRNA transfection (fig. 4e). Cell viability was not significantly different between NBL1 siRNA-transfected DU145 and negative control siRNA-transfected DU145. Next, to determine the possible role of NBL1 in invasiveness, a transwell invasion assay was performed (fig. 4f). Invasion ability 1 day after siRNA transfection was not significantly different between NBL1 siRNA-transfected DU145 and negative control siRNA-transfected DU145.

Discussion

In the present study, we identified several genes that encode secreted proteins present in PCa and NP from CAST libraries. Quantitative RT-PCR revealed that *MSMB*, *NBL1* and *AZGP1* were expressed to a much higher extent in PCa and NP than in 14 types of normal tissues. MSMB, prostatic acid phosphatase and PSA are the three most abundant proteins found in semen. It was reported that MSMB also has high specificity for the prostate and has utility as a serum biomarker for PCa [24]. In addition, a single-nucleotide polymorphism of *MSMB* has been reported to increase the risk of developing PCa [25]. It was also reported that immunohistochemical staining of AZGP1 was a predictor of tumor recurrence and could be used as a specific serum biomarker for PCa [26, 27]. Although we could not detect PSA in our CAST library, we think that PSA might be one of the genes difficult to ligate into the pCAST vector. In contrast, little is known about NBL1 expression in PCa. NBL1 can stimulate differentiation of neuroblastoma cells in culture in the presence of retinoic acid [30], and its growth-suppressive activity has been noted in sarcoma cells [31]. NBL1 may play an important role in preventing cells from entering into the S phase [32]. *NBL1* mRNA was reported to be down-regulated in PCa compared with corresponding NP by quantitative RT-PCR analysis [28, 29].

Because the genes in the present study were identified by CAST analysis of PCa cell lines and quantitative RT-PCR analysis of bulk PCa and NP tissues, immunohistochemical analysis was required to determine which cells expressed these genes. With this analysis, we confirmed that NBL1 was highly expressed in the epithelium of PCa

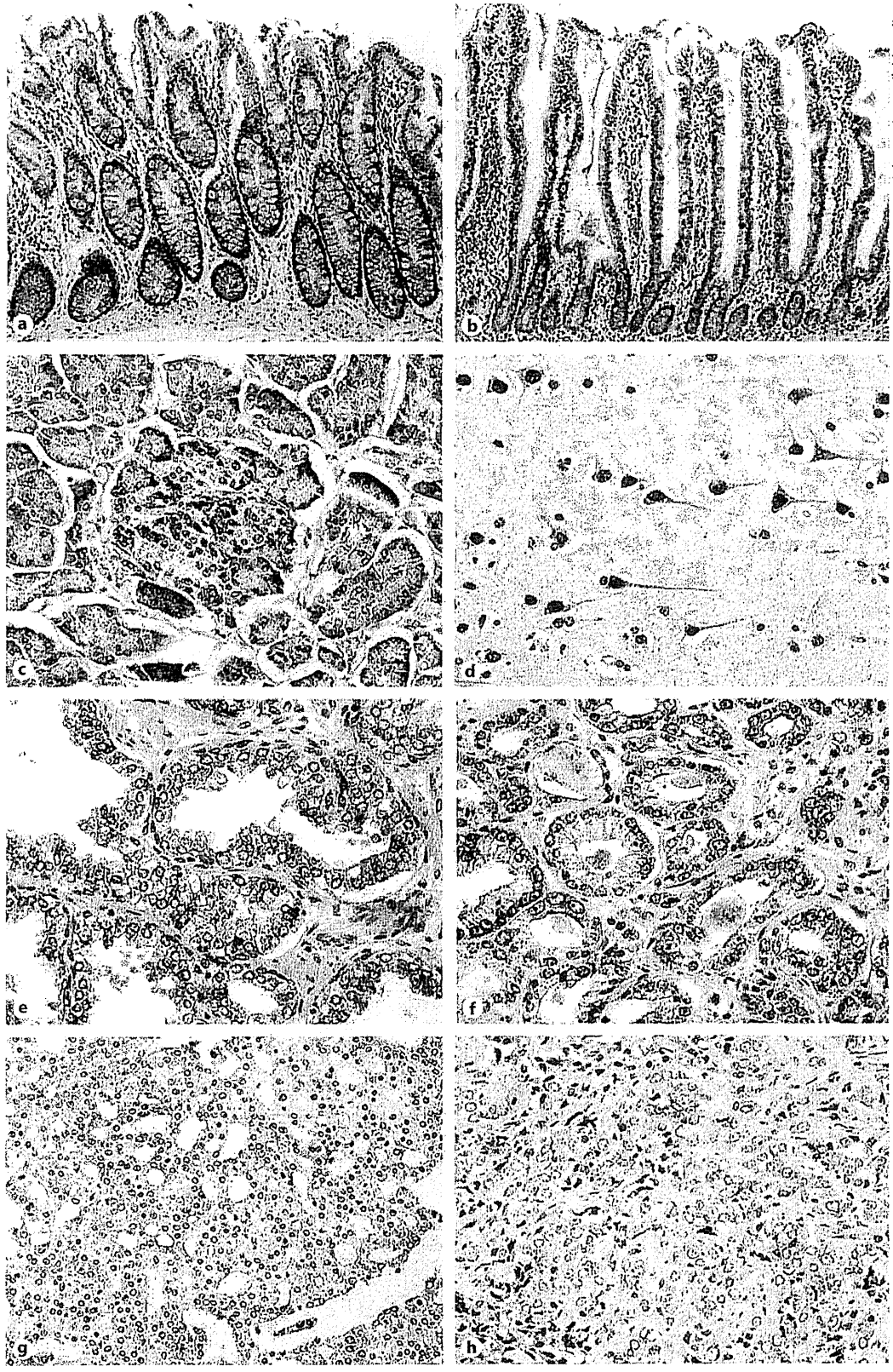

Color version available online

3

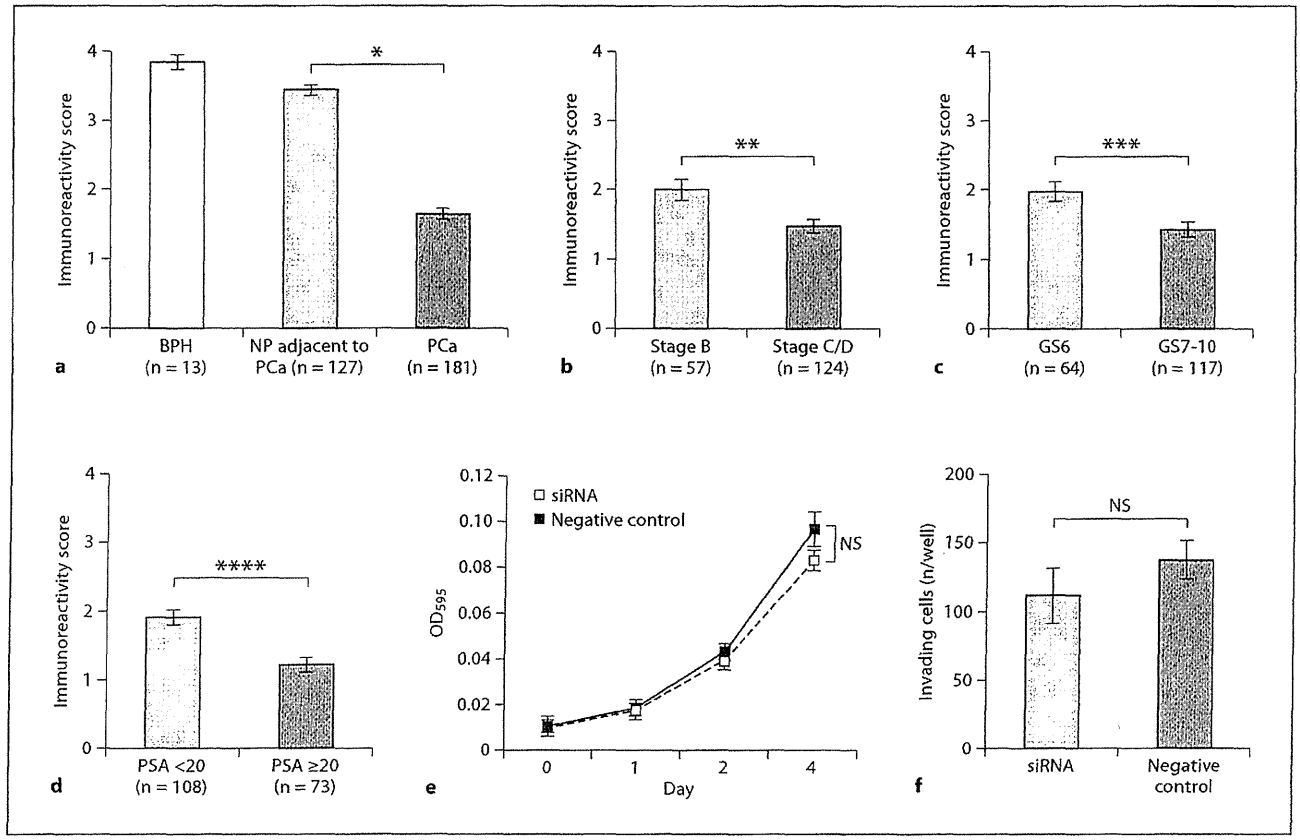

Fig. 4. NBL1 immunoreactivity scores in prostate. NBL1 expression score was higher in NP than in PCa. Means ± SEM. BPH (**a**). NBL1 expression score was higher in stage B than in stages C and D (**b**). NBL1 expression score was higher in PCa with Gleason score 6 than in PCa with Gleason score 7–10 (**c**). NBL1 expression score was higher in PCa with PSA ≤20 than in PCa with PSA >20 (**d**). **e**, **f** Effect of NBL1 knockdown on cell growth (**e**) and cell invasion (**f**) of DU145 cells. **e** Cell growth was assessed by an MTT assay 1, 2 and 4 days after seeding on 96-well plates in DU145 cells. **f** Invading cells were counted after 1 day. Bars and error bars, means and SD of three different experiments. NS = Not significant. * $p < 0.0001$; ** $p = 0.0014$; *** $p = 0.0024$; **** $p < 0.0001$.

and NP. In prostate samples, NBL1 expression was high in NP and lower in PCa. Furthermore, average NBL1 expression was significantly reduced according to the progression of stage, Gleason grade and preoperative PSA value. Because *NBL1* functions as a tumor suppressor gene, these results were consistent with those of previous reports. NBL1 expression was detected in epithelium of the intestine, pancreatic islets and nerve cells, but was absent in other non-cancerous systemic tissues and stromal cells in adult humans. Ozaki et al. [33] examined NBL1 expression in rat tissue by Northern blot analysis and showed that NBL1 was detected in brain, intestine, kidney and lung. They did not test NBL1 expression in rat prostate, but their results were similar to those of our present study in humans.

We also confirmed with Western blot analysis that high NBL1 expression was detected in DU145 cells in culture medium. Nakamura et al. [15] also reported that NBL1 was observed in the culture medium, and the amount of NBL1 secreted from the cells was calculated to be 80% of the total NBL1 protein. Furthermore, NBL1

Fig. 3. Immunohistochemical analysis of NBL1 in non-neoplastic human tissues and prostate tissues. NBL1 expression was detected in the epithelium of the small intestine and colon, islets of the pancreas and nerve cells, respectively (**a–d**). NBL1 staining was observed in the cytoplasm of normal prostate epithelium and PCa cells with Gleason scores 3, 4 and 5, respectively. NBL1 expression was also detected in prostatic ducts (**e–h**).

expression was detected in prostatic ducts in PCa and NP. Therefore, NBL1 may be secreted into semen as well as MSMB, prostatic acid phosphatase and PSA. PSA is produced by secretory epithelial cells in the acini and ducts, and it is secreted directly into the lumen. A characteristic feature of PCa is disruption of the basal cell layer and basement membrane, and this loss of the normal glandular architecture appears to allow PSA increased direct access to the peripheral circulation. PSA is normally found at lower levels in paraurethral and perianal glands, apocrine sweat glands, breast, thyroid and placenta, but these sites do not normally contribute measurable levels of PSA to the circulation [34]. Therefore, in spite of the fact that PSA expression is also higher in NP than in PCa in immunohistochemical analysis, serum PSA is increased in patients with PCa. Although establishment of an enzyme-linked immunosorbent assay system for serum samples is needed to clarify whether NBL1 can serve as a serum marker for detecting and monitoring PCa, we believe that NBL1 might be useful as a serum biomarker for PCa. NBL1 might be beneficial in addition to PSA in situations where PSA is less useful, such as in patients with low PSA level or castration-refractory disease.

The regulation of NBL1 is poorly understood, especially in PCa. Because *NBL1* is thought to be a tumor suppressor gene, it is thought that *NBL1* in PCa has mutations, deletions and methylation. Ozaki et al. [35] reported that two transcription sites were present in the rat NBL1 gene, suggesting the possibility of transcriptional regulation of NBL1. Further studies will clarify how NBL1 is regulated and whether androgen and the androgen receptor axis regulate NBL1. The biological function of the NBL1 protein is also poorly understood in PCa. NBL1 expression correlated with PCa progression, but NBL1 knockdown did not reduce viability and invasiveness relative to the negative control. Because NBL1 was also reported to act as a bone morphogenetic protein (BMP) antagonist by binding to BMPs [36] and BMPs are known to participate in the progression of PCa [37, 38], we speculate that interaction between NBL1 and BMP may play a more important role during growth and development in PCa than in cell cycle inhibition.

In summary, the present study yielded a list of genes that encode secreted proteins present in PCa and NP from CAST analysis. NBL1 expression is narrowly restricted to the prostate and is higher in NP than in PCa. Underexpression of NBL1 is associated with tumor progression. NBL1 has high potential as a biomarker of PCa and its progression.

Acknowledgments

We thank Mr. Shinichi Norimura for his excellent technical assistance and advice. This work was carried out with the kind cooperation of the Research Center for Molecular Medicine, Faculty of Medicine, Hiroshima University. We thank the Analysis Center of Life Science, Hiroshima University, for the provision of their facilities. This work was supported in part by Grants-in-Aid for Cancer Research from the Ministry of Education, Culture, Science, Sports and Technology of Japan; in part by a Grant-in-Aid for the Third Comprehensive 10-Year Strategy for Cancer Control and for Cancer Research from the Ministry of Health, Labor and Welfare of Japan, and in part by a grant (07-23911) from the Princess Takamatsu Cancer Research Fund.

References

1 Yasui W, Oue N, Kitadai Y, Nakayama H: Recent advances in molecular pathobiology of gastric carcinoma; in Kaminishi M, Takubo K, Mafune K (eds): The Diversity of Gastric Carcinoma Pathogenesis: Diagnosis, and Therapy. Tokyo, Springer, 2005, pp 51–71.
2 Yasui W, Oue N, Ito R, Kuraoka K, Nakayama H: Search for new biomarkers of gastric cancer through serial analysis of gene expression and its clinical implications. Cancer Sci 2004;95:385–392.
3 Hayashi T, Oue N, Sakamoto N, et al: Identification of transmembrane protein in prostate cancer by the *Escherichia coli* ampicillin secretion trap: expression of CDON is involved in tumor cell growth and invasion. Pathobiology 2011;78:277–284.
4 Anami K, Oue N, Noguchi T, et al: Search for transmembrane protein in gastric cancer by the *Escherichia coli* ampicillin secretion trap: expression of DSC2 in gastric cancer with intestinal phenotype. J Pathol 2010;221:275–284.
5 Sirovich BE, Schwartz LM, Woloshin S: Screening men for prostate and colorectal cancer in the United States: does practice reflect the evidence? JAMA 2003;289:1414–1420.
6 Boyle P: Screening for prostate cancer: have you had your cholesterol measured? BJU Int 2003;92:191–199.
7 Carter HB: Prostate cancers in men with low PSA levels – must we find them? N Engl J Med 2004;350:2292–2294.
8 Gambert SR: Prostate cancer. When to offer screening in the primary care setting. Geriatrics 2001;56:22–26.
9 Edwards S, Campbell C, Flohr P, et al: Expression analysis onto microarrays of randomly selected cDNA clones highlights HOXB13 as a marker of human prostate cancer. Br J Cancer 2005;92:376–381.
10 Oefelein MG, Resnick MI: Effective testosterone suppression for patients with prostate cancer: is there a best castration? Urology 2003;62:207–213.
11 Chang SS, Kibel AS: The role of systemic cytotoxic therapy for prostate cancer. BJU Int 2009;103:8–17.

12 Ferguson DA, Muenster MR, Zang Q, et al: Selective identification of secreted and transmembrane breast cancer markers using *Escherichia coli* ampicillin secretion trap. Cancer Res 2005;65:8209–8217.
13 von Heijne G: A new method for predicting signal sequence cleavage sites. Nucleic Acids Res 1986;14:4683–4690.
14 Kadonaga JT, Gautier AE, Straus DR, Charles AD, Edge MD, Knowles JR: The role of the beta-lactamase signal sequence in the secretion of proteins by *Escherichia coli*. J Biol Chem 1984;259:2149–2154.
15 Nakamura Y, Ozaki T, Nakagawara A, Sakiyama S: A product of DAN, a novel candidate tumour suppressor gene, is secreted into culture medium and suppresses DNA synthesis. Eur J Cancer 1997;33:1986–1990.
16 Sobin LH, Wittekind CH (eds): TNM Classification of Malignant Tumors, ed 6. New York, Wiley-Liss, 2002, pp 184–187.
17 Eble JN, Sauter G, Epstein JI, et al: World Health Organization Classification of Tumours. Pathology and Genetics of Tumours of the Urinary System and Male Genital Organs. Lyon, IARC Press, 2004.
18 Kondo T, Oue N, Yoshida K, et al: Expression of POT1 is associated with tumor stage and telomere length in gastric carcinoma. Cancer Res 2004;64:523–529.
19 Gibson UE, Heid CA, Williams PM: A novel method for real time quantitative RT-PCR. Genome Res 1996;6:995–1001.
20 Yasui W, Ayhan A, Kitadai Y, et al: Increased expression of p34cdc2 and its kinase activity in human gastric and colonic carcinomas. Int J Cancer 1993;53:36–41.
21 Ohtori S, Yamamoto T, Ino H, et al: Differential screening-selected gene aberrative in neuroblastoma protein modulates inflammatory pain in the spinal dorsal horn. Neuroscience 2002;110:579–586.
22 Sakamoto N, Oue N, Noguchi T, et al: Serial analysis of gene expression of esophageal squamous cell carcinoma: ADAMTS16 is upregulated in esophageal squamous cell carcinoma. Cancer Sci 2010;101:1038–1044.
23 Alley MC, Scudiero DA, Monks A, et al: Feasibility of drug screening with panels of human tumor cell lines using a microculture tetrazolium assay. Cancer Res 1988;48:589–601.
24 Whitaker HC, Warren AY, Eeles R, Kote-Jarai Z, Neal DE: The potential value of microseminoprotein-β as a prostate cancer biomarker and therapeutic target. Prostate 2010;70:333–340.
25 Xu B, Wang J, Tong N, et al: A functional polymorphism in MSMB gene promoter is associated with prostate cancer risk and serum MSMB expression. Prostate 2010;70:1146–1152.
26 Henshall SM, Horvath LG, Quinn DI, et al: Zinc-α_2-glycoprotein expression as a predictor of metastatic prostate cancer following radical prostatectomy. J Natl Cancer Inst 2006;98:1420–1424.
27 Lapointe J, Li C, Higgins JP, et al: Gene expression profiling identifies clinically relevant subtypes of prostate cancer. Proc Natl Acad Sci USA 2004;101:811–816.
28 Asmann YW, Kosari F, Wang K, Cheville JC, Vasmatzis G: Identification of differentially expressed genes in normal and malignant prostate by electronic profiling of expressed sequence tags. Cancer Res 2002;62:3308–3314.
29 Shaikhibrahim Z, Lindstrot A, Buettner R, Wernert N: Analysis of laser-microdissected prostate cancer tissues reveals potential tumor markers. Int J Mol Med 2011;28:605–611.
30 Nakamura Y, Ozaki T, Ichimiya S, Nakagawara A, Sakiyama S: Ectopic expression of DAN enhances the retinoic acid-induced neuronal differentiation in human neuroblastoma cell lines. Biochem Biophys Res Commun 1998;243:722–726.
31 Hanaoka E, Ozaki T, Nakamura Y, Moriya H, Nakagawara A, Sakiyama S: Overexpression of DAN causes a growth suppression in p53-deficient SAOS-2 cells. Biochem Biophys Res Commun 2000;278:20–26.
32 Ozaki T, Nakayama Y, Enomoto H, Hirose M, Sakiyama S: Overexpression of DAN gene product in normal rat fibroblasts causes a retardation of the entry into the S phase. Cancer Res 1995;55:895–900.
33 Ozaki T, Sakiyama S: Molecular cloning and characterization of a cDNA showing negative regulation in v-src-transformed 3Y1 rat fibroblasts. Proc Natl Acad Sci USA 1993;90:2593–2597.
34 Balk SP, Ko YJ, Bubley GJ: Biology of prostate-specific antigen. J Clin Oncol 2003;21:383–391.
35 Ozaki T, Enomoto H, Nakamura Y, et al: The genomic analysis of human DAN gene. DNA Cell Biol 1997;16:1031–1039.
36 Kim AS, Pleasure SJ: Expression of the BMP antagonist Dan during murine forebrain development. Brain Res Dev Brain Res 2003;145:159–162.
37 Hamdy F, Autzen P, Robinson MC, Horne CH, Neal DE, Robson CN: Immunolocalization and messenger RNA expression of bone morphogenetic protein-6 in human benign and malignant prostate tissue. Cancer Res 1997;57:4427–4431.
38 Dai J, Keller J, Zhang J, Lu Y, Yao Z, Keller ET: Bone morphogenetic protein-6 promotes osteoblastic prostate cancer bone metastases through a dual mechanism. Cancer Res 2005;65:8274–8285.

Liver–intestine cadherin induction by epidermal growth factor receptor is associated with intestinal differentiation of gastric cancer

Naoya Sakamoto,[1] Naohide Oue,[1] Kazuhiro Sentani,[1] Katsuhiro Anami,[1] Naohiro Uraoka,[1] Yutaka Naito,[1] Htoo Zarni Oo,[1] Takao Hinoi,[2] Hideki Ohdan,[2] Kazuyoshi Yanagihara,[3] Kazuhiko Aoyagi,[4] Hiroki Sasaki[4] and Wataru Yasui[1,5]

Departments of [1]Molecular Pathology and [2]Surgery, Hiroshima University Graduate School of Biomedical Sciences, Hiroshima; [3]Laboratory of Molecular Cell Biology, Department of Life Sciences, Yasuda Women's University Faculty of Pharmacy, Hiroshima; [4]Division of Genetics, National Cancer Research Institute, Tokyo, Japan

(Received January 27, 2012/Revised May 17, 2012/Accepted May 23, 2012/Accepted manuscript online June 7, 2012/Article first published online July 16, 2012)

Gastric cancer (GC) is one of the most common malignancies worldwide. The epidermal growth factor receptor (EGFR) molecule is very important in GC progression. To examine the correlation between EGFR and GC-related genes, we analyzed gene expression profiles of HT-29 cells treated with EGFR ligands and identified six genes upregulated by epidermal growth factor (EGF) and transforming growth factor (TGF)-α treatment. Among these, we focused on cadherin 17 (*CDH17*) encoding liver–intestine cadherin (LI-cadherin). Expression of LI-cadherin was induced by both EGF and TGF-α, as detected by quantitative RT-PCR and Western blot analysis. A luciferase assay showed that LI-cadherin promoter activity was enhanced by EGF or TGF-α in both HT-29 cells and MKN-74 GC cells. Immunohistochemical analysis of 152 GC cases showed that out of 58 LI-cadherin-positive cases, 24 (41%) cases were also positive for EGFR, whereas out of 94 LI-cadherin-negative cases, only 9 (10%) cases were positive for EGFR ($P < 0.0001$). Double-immunofluorescence staining revealed that EGFR and LI-cadherin were coexpressed. Significant correlation was found between LI-cadherin expression and advanced T grade and N grade. Both EGFR and LI-cadherin expression were more frequently found in GC cases with an intestinal mucin phenotype than in cases with a gastric mucin phenotype. These results indicate that, in addition to the known intestinal transcription factor caudal type homeobox 2, EGFR activation induces LI-cadherin expression and participates in intestinal differentiation of GC. (*Cancer Sci* 2012; 103: 1744–1750)

Gastric cancer remains a major public health issue as the fourth most common cancer and the second leading cause of cancer mortalities worldwide.[1] Gastric cancer is assumed to originate from a sequential accumulation of molecular and genetic alterations to stomach epithelial cells.[2] A molecular understanding of the genetics and epigenetics involved in GC pathogenesis may contribute to identifying novel GC biomarkers and highlight potential avenues for targeted therapies.

Epidermal growth factor and TGF-α both phosphorylate the EGFR and stimulate multiple signaling pathways involved in cell proliferation, anti-apoptosis, and other processes.[3–6] The overexpression of EGF and EGFR by various types of malignancies has been shown to correlate with metastasis, apoptosis, resistance to chemotherapy, and poor prognosis.[5,7,8] We previously reported that both EGF and EGFR are overexpressed in GC, and play a central role in tumor invasion and metastasis through an autocrine mechanism.[9–12] It is therefore important to gain a functional overview of EGFR signaling in GC.

In the present study, we used an oligonucleotide array analysis to generate a list of genes whose expression was induced by TGF-α or EGF treatment, and found that expression of *CDH17* was induced by EGFR ligands. *CDH17* was originally cloned from rat liver in 1994.[13] *CDH17* encodes LI-cadherin protein, which has similarity to the classic cadherins but is structurally distinct. Although the LI-cadherin name derives from the apparent expression pattern of the gene in the rat, in humans LI-cadherin is expressed almost exclusively in the small intestine and colon, but not in the liver.[13] Liver–intestine cadherin is one of the targets of CDX2, the caudal-related homeobox transcription factor. CDX2 has a key role in intestinal development and differentiation, therefore LI-cadherin may play a role in mediating CDX2 function in intestinal cell fate determination. Expression of TGF-α protein is detected in the top one-third of the intestinal crypt, which is composed only of terminally differentiated cells.[14] There are two major phenotypes of GC that are defined according to the mucin expression profile. We previously reported that LI-cadherin expression is associated with an intestinal mucin phenotype.[15] However, induction of gene expression related to intestinal differentiation of GC by EGFR activation has not been investigated. Here, we used luciferase assays to study whether EGFR activation affects *CDH17* transcription. Furthermore, EGFR and LI-cadherin expression were examined in surgically resected GC tissue by immunohistochemistry. The correlation between LI-cadherin expression and clinicopathological characteristics was analyzed.

Materials and Methods

Plasmids. Plasmids used in the present study were generated and described previously.[16] In brief, genomic DNA sequences corresponding to the promoter and 5′-flanking region of the human *CDH17* gene were cloned by PCR using genomic DNA purified from Caco2 cells. The *CDH17* PCR products were subcloned into the pGL4 basic vector (Promega, Madison, MD, USA). Polymerase chain reaction-based approaches were used to introduce mutations in the CDX2 binding sites in the pGL4 basic *CDH17* reporter gene construct. All inserts were verified by automated sequencing.

Cell lines and EGF/TGF-α treatment. The HT-29 colon cancer cell line was obtained from ATCC (Rockville, MD, USA) and maintained in DMEM (Invitrogen, Carlsbad, CA, USA) containing 10% FBS in a humidified atmosphere of 5% CO_2

[5]To whom correspondence should be addressed.
E-mail: wyasui@hiroshima-u.ac.jp

doi: 10.1111/j.1349-7006.2012.02353.x

and 95% air at 37°C. MKN-74 was kindly provided by Dr Toshimitsu Suzuki (Niigata University School of Medicine, Niigata, Japan). HSC-39 and HSC-57 were established by Dr. Kazuyoshi Yanagihara. The cell line HT-29-CDX2 stably expresses CDX2, and HT-29-neo is the control cell line. These cell lines were maintained as described previously.[16] After 24 h of serum starvation, 1–100 nM concentrations of EGF (Sigma, St Louis, MO, USA) or TGF-α were added. The cells were treated for 48 h, and proteins and RNAs were then extracted.

Oligonucleotide array construction, hybridization, detection, and data analysis. The oligonucleotide array, Genopal (Mitsubishi Rayon, Tokyo, Japan), was prepared as described previously.[17] The array contained 208 genes, including GC-related genes identified by our previous SAGE analysis,[18] known genes related to the development and progression of GC,[19,20] genes related to DNA damage response and repair, and genes associated with sensitivity to anticancer drugs.[21] A list of the genes on the array is available upon request. Total RNA isolation, quantification and integrity of RNA assessment, hybridization, detection, and data analysis were carried out as described previously.[22]

Quantitative RT-PCR and Western blot analysis. Quantitative RT-PCR was carried out with an ABI PRISM 7700 Sequence Detection System (Applied Biosystems, Foster City, CA, USA) as described previously.[23] Sequence information of primers for CDX2 and CDH17 is available upon request. The *ACTB*-specific PCR products were amplified from the same RNA samples and served as an internal control. Primer sequences and additional PCR conditions are available upon request.

For Western blot analysis, cells were lysed as described previously.[24] The filter was incubated with primary anti-LI-cadherin antibody (goat polyclonal dilution 1:500 ; Santa Cruz Biotechnology, Santa Cruz, CA, USA). Peroxidase-conjugated anti-goat IgG was used as the secondary probe. Immunocomplexes were visualized with an ECL Western Blot Detection System (Amersham Biosciences, Piscataway, NJ, USA). β-actin antibody (Sigma) was used as a loading control.

Luciferase assay. Forty-eight hours before transfection, cells were plated in 35-mm dishes. Transfection of cells at 30–50% confluency was carried out with 6 μL FuGENE6, 4 μg pGL4 containing LI-cadherin promoter constructs[16] and basic reporter gene construct, and 1 μg phRL-TK Renilla luciferase reporter vector (Promega). At 48 h after transfection, EGF and TGF-α treatment was carried out. At 48 h after treatment, cells were collected and resuspended in reporter lysis buffer (Promega). Luciferase activities were determined with luciferase assay reagent (Promega) and a GloMax luminometer (Promega).

Tissue samples. A total of 152 primary tumor samples were collected from patients diagnosed with GC. Patients were treated at the Hiroshima University Hospital (Hiroshima, Japan) or an affiliated hospital. Tumor staging was according to the TNM classification system. Because written informed consent was not obtained, for privacy protection, identifying information for all samples was removed before analysis. This was in accordance with the Ethical Guidelines for Human Genome/Gene Research of the Japanese Government.

Immunohistochemistry. A Dako LSAB Kit (Dako, Carpinteria, CA, USA) was used for immunohistochemical analysis. In brief, microwave pretreatment in citrate buffer was carried out for 15 min to retrieve antigenicity. After peroxidase activity was blocked with 3% H_2O_2-methanol for 10 min, sections were incubated with normal goat serum (Dako) for 20 min to block non-specific antibody binding sites. Sections were incubated with mouse monoclonal anti-EGFR (1:20; Novocastra, Newcastle, UK) or goat polyclonal anti-LI-cadherin (1:50; Santa Cruz Biotechnology). After a 10-min incubation with substrate–chromogen solution, sections were counterstained with 0.1% hematoxylin. The percentage of stained cancer cells was evaluated for each antibody. A result was considered positive if at least 10% of the cells were stained. When fewer than 10% of cancer cells were stained, the immunostaining was considered negative.

For double-immunofluorescence staining, Alexa Fluor 546-conjugated anti-goat IgG and Alexa Fluor 488-conjugated anti-mouse IgG (Molecular Probes, Eugene, OR, USA) were used as secondary antibodies.

Phenotypic analysis of GC. Gastric cancers were classified into four phenotypes: G type; I type; GI type; and N type. For phenotypic expression analysis of GC, we analyzed immunohistochemistry (as described above) with four antibodies, anti-MUC5AC, anti-MUC6, anti-MUC2, and anti-CD10 (all Novocastra). Gastric cancers in which more than 10% of cells in the section expressed at least one gastric epithelial cell marker (MUC5AC or MUC6) or intestinal epithelial cell marker (MUC2 or CD10) were classified as G type or I type cancers, respectively; sections that showed both gastric and intestinal phenotypes were classified as GI type; and those that lacked both gastric and intestinal phenotypes were classified as N type.

RNA interference and cell growth and *in vitro* invasion assays. To knock down endogenous *CDH17*, RNAi was carried out using *CDH17* and negative control siRNA oligonucleotides (Invitrogen). For MTT assays to monitor cell growth, cells were seeded at 2000 cells per well in 96-well plates.[25] Modified Boyden chamber assays were carried out to examine invasiveness. Transiently transfected cells were plated at 1×10^6 cells per well in RPMI-1640 medium with no serum in the upper chamber of a Transwell insert (8-μm pore diameter; Chemicon, Temecula, CA, USA) coated with Matrigel. Medium containing 10% serum was added in the bottom chamber. After incubation at 37°C for 24 and 48 h, cells in the upper chamber were removed by scraping, and the cells remaining on the lower surface of the insert were stained with CyQuant GR dye (Chemicon, Temecula, CA, USA) to assess the number of cells.

Statistical methods. Correlations between clinicopathologic parameters and LI-cadherin protein expression were analyzed by Fisher's exact test. $P < 0.05$ was considered statistically significant.

Results

Oligonucleotide microarray analysis. To identify GC-related genes whose expression was regulated by EGFR activation, we analyzed the gene expression profiles from TGF-α and EGF-treated HT-29 and non-treated HT-29. Previously, we showed activation of LI-cadherin expression by forced expression of CDX2 in the HT-29 colon cancer cell line;[16] however, in GC cell lines, forced expression of CDX2 could not activate LI-cadherin expression (Naohide Oue, unpublished data, 2010). Therefore, the correlation between EGFR and GC-related genes was investigated in HT-29 cells. Expression levels of 208 individual genes were compared between these two profiles. Six genes were identified that were expressed significantly higher (more than twice) in HT-29 cells treated with TGF-α or EGF, than in non-treated cells (Table 1). In EGFR ligand-treated HT-29 cells, no gene showed lower expression than in non-treated HT-29.

Epidermal growth factor receptor ligands induce LI-cadherin expression. Among six genes whose expression was upregulated in both TGF-α- and EGF-treated cells, we focused on *CDH17*. As shown in Figure 1(a), LI-cadherin expression detected by Western blotting was induced by EGF or TGF-α treatment in both HT-29 and MKN-74 cell lines. It has been

Table 1. Six genes upregulated by both epidermal growth factor (EGF) and transforming growth factor-α (TGF-α) treatment in HT-29 cells

Symbol	Description	Genbank accession no.	Intensity		Fold change	Intensity		Fold change
			No treat	TGF-α		No treat	EGF	
VEGF	Vascular endothelial growth factor	NM_003376.3	3.9	9.1	2.4	3.9	17.3	4.5
CDH17	Cadherin 17, LI cadherin (liver–intestine)	NM_004063	2.7	6.2	2.3	2.7	7.7	2.9
CDKN1A	Cyclin-dependent kinase inhibitor 1A (p21, Cip1)	NM_000389	15.2	39.8	2.6	15.2	41.8	2.7
IL8	Interleukin 8	NM_000584.2	7.7	26.3	3.4	7.7	16.2	2.1
CTSL	Cathepsin L	NM_001912	5.5	14.5	2.6	5.5	11.1	2.0
ABTB2	Ankyrin repeat and BTB (POT) domain containing 2	NM_145804.1	6.3	21.2	3.4	6.3	12.5	2.0

No treat, control cells that did not receive treatment.

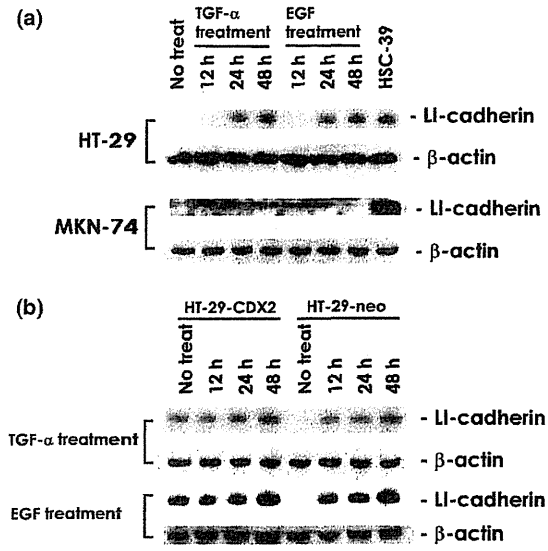

Fig. 1. Induction of liver–intestine cadherin (LI-cadherin) expression in cancer cells treated with epidermal growth factor receptor (EGFR) ligands. (a) LI-cadherin expression in HT-29 and MKN-74 cell lines after epidermal growth factor (EGF)/transforming growth factor-α (TGF-α treatment. (b) LI-cadherin expression in HT29-neo and HT29-caudal type homeobox 2 (CDX2) cell lines after EGF/TGF-α treatment. Western blot analysis confirmed temporal induction of LI-cadherin after EGF/TGF-α treatment, regardless of CDX2 expression.

reported that CDX2 regulates LI-cadherin expression, however, the potential interplay between CDX2 and EGFR signaling pathways has not been investigated. Expression of LI-cadherin in both HT-29-neo and HT-29-CDX2 cell lines was induced after TGF-α or EGF treatment; basal levels of LI-cadherin expression were higher in HT-29-CDX2 than in HT-29-neo cells (Fig. 1b). Quantitative RT-PCR analyses also revealed CDX2 expression was reduced and not induced after treatment with TGF-α or EGF. However, LI-cadherin expression was induced by treatment with TGF-α or EGF (Fig. 2a). A similar tendency was observed in HT-29-neo (data not shown) and HT-29-CDX2 (Fig. 2a) cells. We also examined MUC2, villin, and CD10 expression in HT-29 with TGF-α or EGF treatment. However, induction of these intestinal differentiation markers was not detected. These findings suggest that induction of LI-cadherin expression induced by TGF-α or EGF treatment may occur in a CDX2-independent manner. The induction of LI-cadherin in response to TGF-α or EGF treatment was then studied at a transcriptional level with an LI-cadherin promoter luciferase assay. HT-29 cells were cotransfected with a 0.5-kb human LI-cadherin promoter-driven luciferase construct and an SV40-directed Renilla construct as a control. At 48 h after transfection, cells were stimulated with TGF-α or EGF, resulting in a three and fourfold increase, respectively, in LI-cadherin promoter activity. In our previous observations, four CDX2 binding sites were found in the 0.5-kb human LI-cadherin promoter.[16] We also reported that when human LI-cadherin promoter-driven luciferase constructs with mutations in all four CDX2 binding sites were transfected, luciferase activity was eliminated. To investigate CDX2-independent induction of LI-cadherin by TGF-α or EGF treatment, HT-29 cells were transfected with a LI-cadherin promoter-driven luciferase construct with mutations in all four CDX2 binding sites. Following this transfection, cells stimulated with TGF-α or EGF also showed a three and fourfold increase, respectively, in LI-cadherin promoter activity (Fig. 2b). The similar upregulation of LI-cadherin promoter activity was observed in case of using HT-29-CDX2 (data not shown). We also examined LI-cadherin promoter activity using MKN-74 under the same conditions, and found that cells stimulated with TGF-α or EGF also showed a three and fourfold increase, respectively, in LI-cadherin promoter activity. This implies that EGFR signaling induced LI-cadherin transcription independently of CDX2.

Expression and distribution of EGFR and LI-cadherin in GC tissue. To examine the correlation between EGFR and LI-cadherin expression in GC tissue, we carried out immunohistochemical staining of LI-cadherin and EGFR in 152 surgically resected GC tissue samples. Staining of both LI-cadherin and EGFR occurred at the cell membrane. Of 152 GC cases, LI-cadherin and EGFR were expressed in 58 (38%) and 33 (22%) cases, respectively (Fig. 3a,b). In relation to CDX2, CDX2 expression was observed in almost all LI-cadherin-positive cases, and almost all gastric cancer cells simultaneously expressed CDX2 and LI-cadherin. However, LI-cadherin positive cell contained about a few CDX2 negative cells, CDX2-negative cells frequently expressed EGFR (Fig. 3a–c). In light of these findings, we suspect that EGFR contribute to induce LI-cadherin expression in GC at least partially. Coexpression of LI-cadherin and EGFR was observed in some GC cells by double-immunofluorescence staining (Fig. 3d). In EGFR-positive GC cells, expression of LI-cadherin was frequently found. However, in LI-cadherin-positive GC cells, EGFR was not always detected. In total, of 33 EGFR-positive cases, 24 (73%) cases were LI-cadherin-positive, whereas of 119 EGFR-negative cases, only 34 (29%) cases were LI-cadherin-positive ($P < 0.0001$, Table 2).

Clinicopathological characteristics of LI-cadherin-positive and EGFR-positive GC. The relationship of LI-cadherin staining to clinicopathological characteristics were investigated (Table 3). The LI-cadherin staining was observed more

doi: 10.1111/j.1349-7006.2012.02353.x

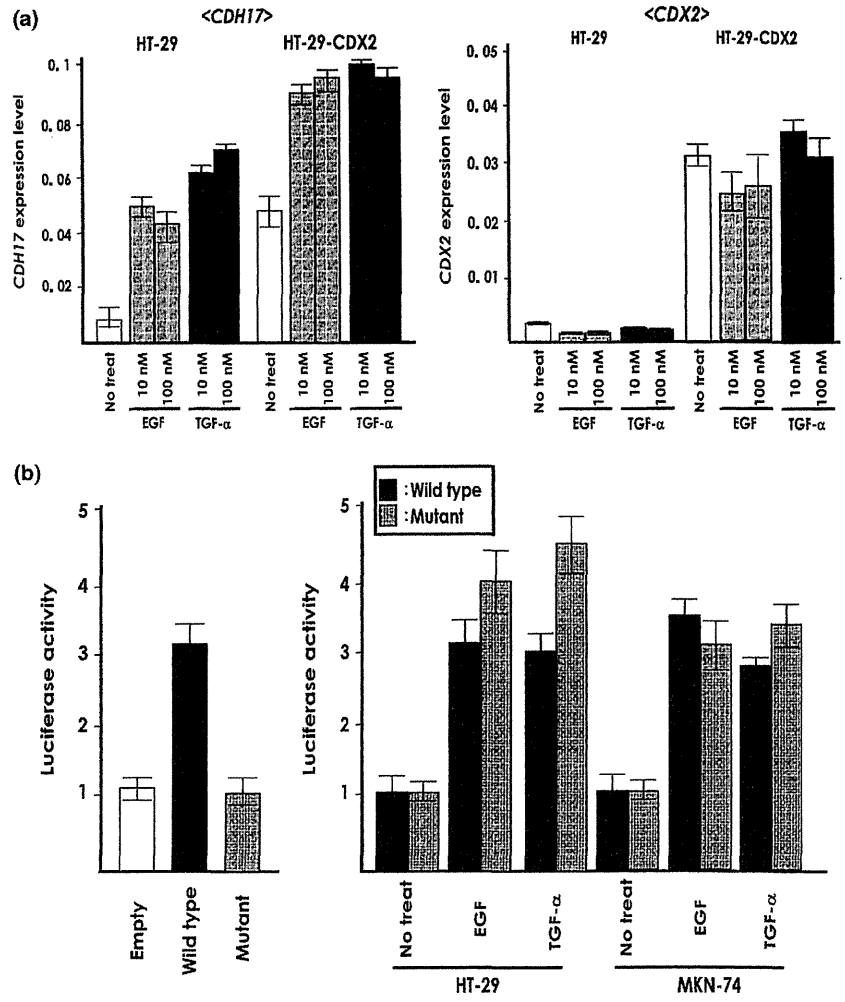

Fig. 2. Effect of epidermal growth factor (EGF)/transforming growth factor-α (TGF-α) treatment on cadherin 17 (*CDH17*) and caudal type homeobox 2 (*CDX2*) expression. (a) Quantitative RT-PCR analysis. Strong induction of *CDH17* was observed in both HT-29 and HT-29-CDX2 cells after EGF or TGF-α treatment without the upregulation of *CDX2*. (b) Liver–intestine cadherin (LI-cadherin) promoter reporter assays. Bars and error bars, mean and SE, respectively, of three different experiments. No treat, negative control. In the right-hand graph, luciferase activity of EGF and TGF-α were standardized by normalizing the strain that did not receive treatment (no treat) at 1.0. Empty, empty vector transfected HT-29 cells; Mutant, HT-29 or MKN-74 transfected with a LI-cadherin promoter-driven luciferase construct with mutations in all four CDX2 binding sites; Wild type, HT-29 or MKN-74 transfected with a LI-cadherin promoter-driven luciferase construct with no mutations in all CDX2 binding sites.

frequently in stage I/II cases (16/41, 39%) than in stage III/IV cases (6/39, 15%; $P = 0.0243$, Fisher's exact test). Moreover, LI-cadherin staining was detected more frequently in intestinal-type GC (20/46, 46%) than in diffuse-type GC (2/34, 6%; $P < 0.0001$, Fisher's exact test). In addition to the Lauren histology-based classification, GC can be subdivided into four phenotypes according to mucin expression. Gastric and intestinal markers were detected in 67 of 152 (44%) cases for MUC5AC, 16 (11%) cases for MUC6, 46 (31%) cases for MUC2, and 16 (11%) cases for CD10. We further investigated the association between LI-cadherin expression and mucin phenotype, because LI-cadherin was detected in intestinal metaplasia of the stomach and colon. Expression of both EGFR and LI-cadherin was found more frequently in GC of I and GI types than GC of G and GI types (Fig. 3d). In the group of 59 advanced GC patients, EGFR expression had significant prognostic impact. However, no significant prognostic impact was found for LI-cadherin expression in GC cases (data not shown).

Effect of LI-cadherin inhibition on cell growth and invasive activity. The LI-cadherin-positive GC cases were observed more frequently in stage III/IV than in stage I/II, suggesting that LI-cadherin could be associated with tumor progression. However, the biological significance of LI-cadherin in GC has not been studied. We carried out an MTT assay 8 days after LI-cadherin siRNA transfection in the HSC-57 cell line. HSC-57 cells were selected for high LI-cadherin expression. We confirmed that LI-cadherin siRNA-transfected HSC-57 cells showed significantly reduced LI-cadherin expression (data not shown). Cell viability was not significantly different between LI-cadherin siRNA-transfected and negative control GC cells (data not shown). To determine the possible role of LI-cadherin in GC cell invasiveness, a Transwell invasion assay was carried out in the HSC-57 cell line. There was no significant difference in invasion between LI-cadherin knockdown and negative control GC cells (data not shown).

Discussion

In the present study, by using a customized oligonucleotide microarray, we identified six GC-related genes (*VEGF*, *CDH17*, *CDKN1*, *IL8*, *CTSL*, and *ABTB2*) whose expression was upregulated by EGFR activation. Among these genes, we successfully showed that EGFR activation induced LI-cadherin expression. In addition, LI-cadherin induction occurred in a CDX2-independent manner, and additional induction of LI-cadherin expression was observed in CDX2-transfected cells. These results suggest that high expression of LI-cadherin is required for EGFR activation as well as CDX2 expression. Because the EGFR signaling pathway forms a wide-ranging network, it remains unclear which component of the signaling pathway directly regulates LI-cadherin. This requires further study.

In normal colon, expression of EGFR and LI-cadherin was found. Both TGF-α and $p21^{waf1/cip1}$ protein expression is only detected in the top one-third of the crypt, which is only composed of terminally differentiated cells.[26,27] In the present study, expression of $p21^{waf1/cip1}$ was also induced by TGF-α

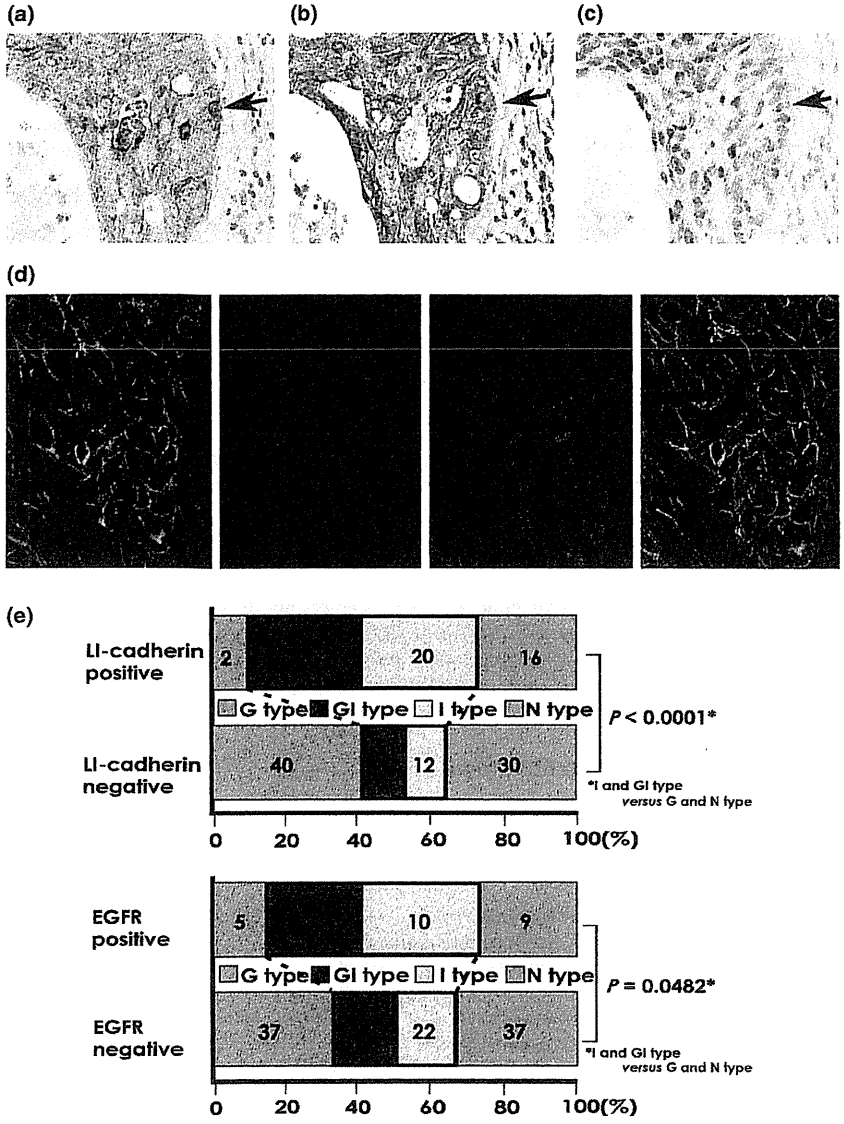

Fig. 3. Immunohistochemical analysis of epidermal growth factor receptor (EGFR) and liver–intestine cadherin (LI-cadherin) in gastric cancer (GC) and phenotypic analysis of EGFR- and LI-cadherin-positive GC cases. Expression pattern of EGFR (a), caudal type homeobox 2 (CDX2) (b), and LI-cadherin (c) (original magnification, ×400). Arrows indicate EGFR-positive (a), LI-cadherin-positive (b), and CDX2-negative (c) GC cells. (d) Double immunofluorescence staining shows that EGFR and LI-cadherin were coexpressed in some GC cells. Blue, DAPI; green, EGFR; red, LI-cadherin. (e) Distribution of gastric (G), intestinal (I), gastric and intestinal mixed (GI), and unclassified (N) phenotypes of GC in EGFR- and LI-cadherin-positive cases. Both EGFR and LI-cadherin expression were more frequently found in GC with intestinal features (I or GI type) than the others. *P*-values were analyzed by Fisher's exact test.

Table 2. Expression of liver–intestine cadherin (LI-cadherin) and epidermal growth factor receptor (EGFR) in gastric cancer tissue

	EGFR		*P*-value†
	Positive	Negative	
LI-cadherin			
Positive	24	34	<0.0001
Negative	9	85	

†Fisher's exact test.

and EGF treatment (data not shown). It has been reported that $p21^{waf1/cip1}$ is associated with the processes of cell-cycle arrest, apoptosis, and differentiation.[28] Taken together, these results suggest that EGFR activation induces intestinal differentiation. High expression of LI-cadherin may have some effect on terminal differentiation of colonic epithelial cells. However, despite induction of $p21^{waf1/cip1}$ expression, cell growth activity was upregulated in HT-29 cells (data not shown). To clarify whether $p21^{waf1/cip1}$ is involved in cell growth inhibition of HT-29, further studies are required.

In GC, LI-cadherin overexpression has been reported to be associated with lymph node metastasis.[29] In contrast, in colorectal cancer, reduced expression of LI-cadherin is frequently found in cases with lymph node metastasis or poor survival. Thus, the functions of LI-cadherin in human cancers are controversial and unclear. In the present study, we carried out MTT and Transwell invasion assays after LI-cadherin knockdown in the HSC-57 cell line. However, cell viability and invasion ability were not significantly altered. To clarify the biological and clinical significance of EGFR and LI-cadherin expression in GC, we examined the expression of these two molecules in GC tissue through immunohistochemistry and compared this with clinicopathologic parameters, prognosis, and mucin phenotype. Our data for the relation between molecular expression and tumor stage in all of our GC cases were consistent with the results of previous studies.[30] With regard to mucin phenotype, both EGFR and LI-cadherin expression were detected more frequently in I-type GC, and this finding is in accordance with previous studies.[15] Many studies have implicated the EGFR signaling pathway in the regulation of intestinal epithelial cell growth and differentiation.[31–33] Animals that are EGFR-null die early in postnatal life and show severe defects in intestinal cell proliferation and organization, along with many other abnormalities.[31] Overexpression or mutation of EGFR has been associated with many different carcinomas, including colonic carcinoma.[34] These

doi: 10.1111/j.1349-7006.2012.02353.x

Table 3. Relationship between liver–intestine cadherin (LI-cadherin) or epidermal growth factor receptor (EGFR) and clinicopathologic characteristics of gastric cancer

	LI-cadherin			EGFR		
	Positive (%)	Negative	*P*-value†	Positive (%)	Negative	*P*-value†
T grade						
T1	10 (23)	33	0.0254	0 (0)	43	<0.0001
T2/3/4	48 (44)	51		33 (30)	76	
N grade						
N0	17 (27)	46	0.0186	6 (10)	57	0.0025
N1/2/3	41 (46)	48		27 (30)	62	
Stage						
I/II	25 (31)	55	0.0689	10 (13)	70	0.0054
III/IV	33 (46)	39		23 (32)	49	
Histology						
Intestinal	33 (43)	43	0.2424	11 (14)	65	0.0481
Diffuse	25 (33)	51		22 (29)	54	

†Fisher's exact test.

observations indicate that the EGFR signaling pathway plays an important role in regulating intestinal epithelial cell production. In the light of these previous studies and ours, it is suspected that EGFR drives GC development through wide-ranging signaling pathways, and also induces intestinal phenotypes in GC by stimulation of LI-cadherin expression.

In summary, this study yielded a list of genes that were upregulated by EGFR activation in GC. We found that LI-cadherin is induced by EGFR, and overexpression of LI-cadherin is associated with the intestinal mucin phenotype. These results suggest that, in addition to CDX2, EGFR activation is involved in LI-cadherin expression in GC, and that EGFR may induce intestinal differentiation through upregulating LI-cadherin expression in a CDX2-independent manner.

Acknowledgments

We thank Mr Shinichi Norimura for his excellent technical assistance and advice. This work was carried out with the kind cooperation of the Research Center for Molecular Medicine, Faculty of Medicine, Hiroshima University (Hiroshima, Japan). We thank the Analysis Center of Life Science, Hiroshima University, for the use of their facilities. This work was supported in part by Grants-in-Aid for Cancer Research from the Ministry of Education, Culture, Science, Sports, and Technology of Japan, in part by a Grant-in-Aid for the Third Comprehensive 10-Year Strategy for Cancer Control and for Cancer Research from the Ministry of Health, Labor and Welfare of Japan, and in part by a grant (07-23911) from the Princess Takamatsu Cancer Research Fund.

Disclosure Statement

The authors have no conflict of interest.

Abbreviations

CDH17	cadherin 17
CDX2	caudal type homeobox 2
EGF	epidermal growth factor
EGFR	epidermal growth factor receptor
G type	gastric type
GC	gastric cancer
GI type	gastric and intestinal mixed type
I type	intestinal type
LI-cadherin	liver–intestine cadherin
N type	unclassified type
TGF-α	transforming growth factor-α

References

1 Crew KD, Neugut AI. Epidemiology of gastric cancer. *World J Gastroenterol* 2006; **12**: 354–62.
2 Yasui W, Sentani K, Sakamoto N, Anami K, Naito Y, Oue N. Molecular pathology of gastric cancer: research and practice. *Pathol Res Pract* 2011; **207**: 608–12.
3 Kang MJ, Ryu BK, Lee MG *et al.* NF-kappaB activates transcription of the RNA-binding factor HuR, via PI3K-AKT signaling, to promote gastric tumorigenesis. *Gastroenterology* 2008; **135**: 2030–42.
4 Regalo G, Resende C, Wen X *et al.* C/EBP alpha expression is associated with homeostasis of the gastric epithelium and with gastric carcinogenesis. *Lab Invest* 2010; **90**: 1132–9.
5 Yu HG, Ai YW, Yu LL *et al.* Phosphoinositide 3-kinase/Akt pathway plays an important role in chemoresistance of gastric cancer cells against etoposide and doxorubicin induced cell death. *Int J Cancer* 2008; **122**: 433–43.
6 Yamamoto H, Kitadai Y, Yamamoto H *et al.* Laminin gamma2 mediates Wnt5a-induced invasion of gastric cancer cells. *Gastroenterology* 2009; **137**: 242–52.
7 Mitani Y, Oue N, Matsumura S *et al.* Reg IV is a serum biomarker for gastric cancerpatients and predicts response to 5-fluorouracil-based chemotherapy. *Oncogene* 2007; **26**: 4383–93.
8 Tahara E, Sumiyoshi H, Hata J *et al.* Human epidermal growth factor in gastric carcinoma as a biologic marker of high malignancy. *Jpn J Cancer Res* 1986; **77**: 145–52.
9 Yasui W, Hata J, Yokozaki H *et al.* Interaction between epidermal growth factor and its receptor in progression of human gastric carcinoma. *Int J Cancer* 1988; **41**: 211–17.
10 Yasui W, Sumiyoshi H, Hata J *et al.* Expression of epidermal growth factor receptor in human gastric and colonic carcinomas. *Cancer Res* 1988; **48**: 137–41.
11 Ito R, Kitadai Y, Kyo E *et al.* Interleukin 1 alpha acts as an autocrine growth stimulator for human gastric carcinoma cells. *Cancer Res* 1993; **53**: 4102–6.
12 Yoshida K, Tsujino T, Yasui W *et al.* Induction of growth factor-receptor and metalloproteinase genes by epidermal growth factor and/or transforming growth factor-alpha in human gastric carcinoma cell line MKN-28. *Jpn J Cancer Res* 1990; **81**: 793–8.
13 Berndorff D, Gessner R, Kreft B *et al.* Liver-intestine cadherin: molecular cloning and characterization of a novel Ca(2+)-dependent cell adhesion molecule expressed in liver and intestine. *J Cell Biol* 1994; **125**: 1353–69.
14 Sheng G, Bernabe KQ, Guo J, Warner BW. Epidermal growth factor receptor-mediated proliferation of enterocytes requires p21waf1/cip1 expression. *Gastroenterology* 2006; **131**: 153–64.

15 Motoshita J, Nakayama H, Taniyama K, Matsusaki K, Yasui W. Molecular characteristics of differentiated-type gastric carcinoma with distinct mucin phenotype: LI-cadherin is associated with intestinal phenotype. *Pathol Int* 2006; **56**: 200–5.
16 Hinoi T, Lucas PC, Kuick R, Hanash S, Cho KR, Fearon ER. CDX2 regulates liver intestine-cadherin expression in normal and malignant colon epithelium and intestinal metaplasia. *Gastroenterology* 2002; **123**: 1565–77.
17 Nagao K, Togawa N, Fujii K *et al.* Detecting tissue-specific alternative splicing and disease-associated aberrant splicing of the PTCH gene with exon junction microarrays. *Hum Mol Genet* 2005; **14**: 3379–88.
18 Oue N, Hamai Y, Mitani Y *et al.* Gene expression profile of gastric carcinoma: identification of genes and tags potentially involved in invasion, metastasis, and carcinogenesis by serial analysis of gene expression. *Cancer Res* 2004; **64**: 2397–405.
19 Hasegawa S, Furukawa Y, Li M *et al.* Genome-wide analysis of gene expression in intestinal-type gastric cancers using a complementary DNA microarray representing 23,040 genes. *Cancer Res* 2002; **62**: 7012–17.
20 Inoue H, Matsuyama A, Mimori K, Ueo H, Mori M. Prognostic score of gastric cancer determined by cDNA microarray. *Clin Cancer Res* 2002; **8**: 3475–9.
21 Zembutsu H, Ohnishi Y, Tsunoda T *et al.* Genome-wide cDNA microarray screening to correlate gene expression profiles with sensitivity of 85 human cancer xenografts to anticancer drugs. *Cancer Res* 2002; **62**: 518–27.
22 Oue N, Sentani K, Sakamoto N *et al.* Characteristic gene expression in stromal cells of gastric cancers among atomic-bomb survivors. *Int J Cancer* 2009; **124**: 1112–21.
23 Kondo T, Oue N, Yoshida K *et al.* Expression of POT1 is associated with tumor stage and telomere length in gastric carcinoma. *Cancer Res* 2004; **64**: 523–9.
24 Yasui W, Sano T, Nishimura K *et al.* Expression of P-cadherin in gastric carcinomas and its reduction in tumor progression. *Int J Cancer* 1993; **54**: 49–52.
25 Alley MC, Scudiero DA, Monks A *et al.* Feasibility of drug screening with panels of human tumor cell lines using a microculture tetrazolium assay. *Cancer Res* 1988; **48**: 589–601.
26 Xian CJ, Mardell CE, Read LC. Specificity of the localization of transforming growth factor-alpha immunoreactivity in colon mucosa. *J Histochem Cytochem* 1999; **47**: 949–58.
27 Sinicrope FA, Roddey G, Lemoine M *et al.* Loss of p21WAF1/Cip1 protein expression accompanies progression of sporadic colorectal neoplasms but not hereditary nonpolyposis colorectal cancers. *Clin Cancer Res* 1998; **4**: 1251–61.
28 Abbas T, Dutta A. p21 in cancer: intricate networks and multiple activities. *Nat Rev Cancer* 2009; **9**: 400–14.
29 Park SS, Kang SH, Park JM *et al.* Expression of liver-intestine cadherin and its correlation with lymph node metastasis in gastric cancer: can it predict N stage preoperatively? *Ann Surg Oncol* 2007; **14**: 94–9.
30 Ito R, Oue N, Yoshida K *et al.* Clinicopathological significant and prognostic influence of cadherin-17 expression in gastric cancer. *Virchows Arch* 2005; **447**: 717–22.
31 Miettinen PJ, Berger JE, Meneses J *et al.* Epithelial immaturity and multiorgan failure in mice lacking epidermal growth factor receptor. *Nature* 1995; **376**: 337–41.
32 Barnard JA, Beauchamp RD, Russell WE, Dubois RN, Coffey RJ. Epidermal growth factor-related peptides and their relevance to gastrointestinal pathophysiology. *Gastroenterology* 1995; **108**: 564–80.
33 Abud HE, Watson N, Heath JK. Growth of intestinal epithelium in organ culture is dependent on EGF signalling. *Exp Cell Res* 2005; **303**: 252–62.
34 Salomon DS, Brandt R, Ciardiello F, Normanno N. Epidermal growth factor-related peptides and their receptors in human malignancies. *Crit Rev Oncol Hematol* 1995; **19**: 183–232.

doi: 10.1111/j.1349-7006.2012.02353.x

Journal of Crohn's and Colitis (2012) 6, 425–434

Available online at www.sciencedirect.com

SciVerse ScienceDirect

Olfactomedin-4 is a glycoprotein secreted into mucus in active IBD☆

Michael Gersemann [a, b,*], Svetlana Becker [b], Sabine Nuding [b], Lena Antoni [b], German Ott [c], Peter Fritz [c], Naohide Oue [d], Wataru Yasui [d], Jan Wehkamp [a, b], Eduard F. Stange [a]

[a] *Department of Internal Medicine I, Robert Bosch Hospital, Stuttgart, Germany*
[b] *Dr. Margarete Fischer-Bosch Institute of Clinical Pharmacology, Stuttgart and University of Tübingen, Germany*
[c] *Department of Pathology, Robert Bosch Hospital, Stuttgart, Germany*
[d] *Department of Molecular Pathology, Hiroshima University Graduate School of Biomedical Science, Hiroshima, Japan*

Received 12 August 2011; received in revised form 28 September 2011; accepted 28 September 2011

KEYWORDS
Inflammatory bowel disease;
Olfactomedin-4;
Intestinal stem cell marker;
Defensins;
Mucins;
Mucus

Abstract

Background: Olfactomedin-4 (OLFM4) is a glycoprotein characteristic of intestinal stem cells and apparently involved in mucosal defense of the stomach and colon. Here we studied its expression, regulation and function in IBD.
Methods: The expression of OLFM4, mucins Muc1 and Muc2, the goblet cell differentiation factor Hath1 and the proinflammatory cytokine IL-8 was measured in inflamed or noninflamed colon in IBD patients and controls. OLFM4 protein was located by immunohistochemistry, quantified by Dot Blot and its binding capacity to defensins HBD1-3 was investigated. The influence of bacteria with or without the Notch blocker dibenzazepine (DBZ) and of several cytokines on OLFM4 expression was determined in LS174T cells.
Results: OLFM4 mRNA and protein were significantly upregulated in inflamed CD (4.3 and 1.7-fold) and even more pronounced in UC (24.8 and 3.7-fold). OLFM4 expression was correlated to IL-8 but not to Hath1. In controls immunostaining was restricted to the lower crypts but in inflamed IBD it expanded up to the epithelial surface including the mucus. OLFM4 bound to HBD1-3 without profoundly inactivating these defensins. In LS174T-cells OLFM4 mRNA was significantly augmented after incubation with *Escherichia coli K12*, *Escherichia coli Nissle* and *Bacteroides vulgatus*. DBZ downregulated OLFM4 expression and blocked bacterial induction whereas IL-22 but not TNF-α was stimulatory.

☆ Conference presentation: DDW 2011, Chicago, USA (poster).

* Corresponding author at: Robert Bosch Hospital, Internal Medicine I, Auerbachstr. 110, D-70376 Stuttgart, Germany. Tel.: +49 711 81015912; fax: +49 711 81013793.
E-mail address: michael.gersemann@rbk.de (M. Gersemann).

1873-9946/$ - see front matter
doi:10.1016/j.crohns.2011.09.013

Conclusions: OLFM4 is overexpressed in active IBD and secreted into mucus. The induction is triggered by bacteria through the Notch pathway and also by the cytokine IL-22. OLFM4 seems to be of functional relevance in IBD as a mucus component, possibly by binding defensins.

1. Introduction

In both inflammatory bowel diseases (IBD) the chronic inflammation is mediated by an immune response directed against commensal bacteria, possibly triggered by a disproportionate immune response toward these microbes that damages the mucosa.[1] On the other hand, there is increasing evidence for a primary role of a defective mucosal barrier in Crohn's disease (CD) and ulcerative colitis (UC).[2–4] Bacteria from the lumen massively contaminate the mucus layer[5] which is normally sterile in the bottom stratum.[6] Some bacteria are epithelial adherent[5,7] or may even invade the subepithelial space[5,8] and thus trigger an immune response.

The mucosal barrier is a multilayer structure composed of the mucus layer[6] and its origin, the epithelium. In the large intestine the key secretory cells are the goblet cells. They produce various mucins forming the mucus layer which is acting as a physical and chemical barrier against commensals and pathogens.[9] The colonic epithelium also produces antimicrobial peptides which are ultimately secreted into the mucus.[10,11] The more important colonic peptides, the ß-defensins, are characterized by a broad antimicrobial activity against a variety of gram-positive and gram-negative bacteria preventing luminal microbes to enter the lower mucus layer and attack the epithelium.[12]

This intestinal protective barrier mediated by mucus and defensins is disturbed in IBD. In CD, the expression of the antimicrobial peptides is compromised enabling the bacteria to invade the mucosa and thus trigger inflammation.[3,13] In case of colonic involvement, CD is linked to a diminished expression of HBD1 independent of inflammation.[14] In UC, the mucus layer is thinner than normal and may even be missing.[15,16] This is accompanied by a diminished mucin synthesis,[17–21] which is apparently related to a failure in the differentiation of intestinal stem cells toward goblet cells.[17] This differentiation is governed by the key transcription factor Hath1 which is correlated with mucin synthesis.[17]

Olfactomedin-4 (OLFM4) is an olfactomedin domain-containing protein which was found preferentially in the human gastrointestinal tract.[22–24] The function of OLFM4 in the digestive tract is probably complex. OLFM4 may be an important part of the gastrointestinal mucosal surface and therefore play a role in its defense.[25] For instance, OLFM4 is known to create large polymers stabilized by disulfide bonds,[25] similar to mucins.[9] Moreover, it was demonstrated to interact with cell surface cadherin and lectins facilitating cell adhesion.[26] A role of OLFM4 in epithelial defense was concluded from an upregulation in a mouse primary gastric epithelial cell line GSM06 incubated with *Helicobacter pylori*,[27] as well as in *H. pylori* infected patients in vivo.[28] Finally, in addition to LGR5[29] also OLFM4 was found to be a small and large intestinal marker for crypt stem cells in humans.[30]

However, little is known about its relevance in the colon. Shinozaki et al. found OLFM4 transcripts to be significantly upregulated in the epithelium in active vs. inactive UC but its precise function remained unclear.[31] In the present study we attempted to better define the role of OLFM4 in the pathogenesis of IBD and suggest that this peptide acts as an inflammation induced mucus component binding defensins.

2. Material and methods

2.1. Patients

The diagnosis of CD and UC was based on classical clinical, radiological and endoscopic findings.[32,33] Endoscopic biopsies were immediately snap-frozen in liquid nitrogen. All patients gave their written informed consent and the study was approved by the ethical committee of the University of Tübingen (Germany).

For real-time PCR analysis biopsies from the colonic sigma were obtained in a total of 160 individuals, who underwent routine colonoscopy for various indications, such as colon cancer screening, IBD, diarrhea or obstipation. Thirty-three of these biopsies were classified as healthy controls, 72 were from CD patients (36 noninflamed and 36 inflamed samples) and 55 had the diagnosis of UC (28 noninflamed and 27 inflamed samples). All samples were collected at the Robert Bosch Hospital (Stuttgart, Germany) and the intensity of the flare was clinically evaluated in these patients using the Colitis Activity Index (CAI) for UC and the Crohn's disease activity index (CDAI) for CD.

Immunostaining was performed in formalin-fixed or Carnoy-fixed paraffin-embedded colonic tissue. A total of 18 formalin-fixed colonic resections (6 controls, 6 inflamed CD and 6 inflamed UC samples) and 10 Carnoy-fixed rectal biopsies (5 inflamed CD and 5 inflamed UC samples) were investigated. For Dot Blot analysis, sigma biopsies of 4 controls, 4 inflamed CD and 4 inflamed UC patients, as well as mucus extracts obtained by colonoscopic brushings from 3 controls, 3 inflamed CD and 3 inflamed UC samples were collected. Brushings were performed by gently scrubbing the rectal mucosa with an endoscopic brush, removing the endoscope from the rectum and, outside the patient, the brush was cut with scissors and snap frozen in liquid nitrogen.

2.2. RNA isolation and reverse transcription

The frozen tissues were mechanically disrupted and total RNA was isolated using TRIzol reagent (Invitrogen, Karlsruhe, Germany). RNA quality was checked with the Agilent RNA 6000 Nano Kit (Agilent Technologies, Santa Clara, CA, USA). 500 ng of total RNA was reverse transcribed with AMV reverse transcriptase according to the supplier's protocol

(Promega, Mannheim, Germany). RNA preparations were used for real-time PCR analysis.

2.3. Protein preparation

Frozen sigmoid biopsies were pulverized with a pestle in liquid nitrogen. Proteins were extracted under gentle agitation for 90 min diluted in 100 µl homogenization buffer (50 mM Tris HCl, 250 mM sucrose, 1 mM EDTA, pH 7.6). Extracts were centrifuged for 20 min (13200 g, 4 °C) and the supernatants were immediately snap-frozen in liquid nitrogen. Mucus extracts were incubated for 2 h in 300 µl 5% acetic acid following a centrifugation for 10 min (7000 g, 4 °C). Then the supernatants were extracted and dried in a vacuum concentrator. Pellets were diluted in 80 µl 0.01% acetic acid and immediately snap-frozen in liquid nitrogen. Protein content in biopsies and mucus extracts was measured using a Bicinchoninic Acid Protein Assay (Smith) as described previously.[34] Isolated proteins were used for Dot Blot analyses.

2.4. Quantitative real-time reverse transcriptase PCR

For mRNA quantification, real-time PCR was carried out in a SYBR Green fluorescence temperature cycler (LightCycler®, Roche Diagnostics, Mannheim, Germany). Single-stranded cDNA (or gene-specific plasmids as controls) corresponding to 10 ng of RNA conducted as a template with specific oligonucleotide primer pairs (Table 1) as described previously.[13] All primers were tested for specific binding to the sequence of interest using BLAST. Plasmids for each product were generated with the TOPO TA Cloning Kit (Invitrogen, Carlsbad, CA, USA) according to the supplier's protocol. PCR-amplified DNA fragments were confirmed by sequencing. Internal standard curves were produced by serial dilution of the correctly sequenced plasmids. The mRNA data were normalized to ß-actin mRNA.

2.5. Immunohistochemistry

A monoclonal antibody directed against OLFM4 (N212) was produced by W.Y. in the Department of Molecular Pathology, Hiroshima University Graduate School of Biomedical Science, Hiroshima, Japan; proof for its specificity has previously been published.[35] Immunostaining for OLFM4 was performed using a two-step immunoperoxidase technique (EnVision™, Dako, Glostrup, Denmark) as described previously.[36] Antigen retrieval was performed by heating for 30 min in a steamer (pH 9). Then, sections were incubated for 1 h with the primary anti-OLFM4 antibody diluted 1:100 in TBST (20 mM Tris-Base (pH 7.4), 0.14 M NaCl, 0.1% Tween 20). Visualization was performed using a detection kit as outlined by the supplier (Dako, Glostrup, Denmark: horse-radish-peroxidase (HRP)-labeled secondary antibody, detection with 3'-diaminobenzidine tetrahydrochloride). Sections were counterstained with hematoxylin. The grade of inflammation was blindly evaluated in H & E stained sections by an experienced pathologist blinded to the immunohistochemical and molecular biological results.

2.6. Dot Blot analysis

The specificity of the anti-OLFM4 antibody (N212) was tested in Western Blot experiments using human sigma biopsies. We found a clear signal at 57 kDa in inflamed UC samples which is less intense in inflamed CD and uninflamed controls (data not shown). Due to the limited protein amounts obtained by a single biopsy, we decided to switch to the Dot Blot technique which needs less total protein amounts as compared to the Western Blot. Therefore, 10 µg of total protein was transferred to 0.45 mg pore size nitrocellulose membranes (Schleicher & Schuell, Keene, NH, USA) and blocked with 5% skimmed milk powder in TBST for 1 h. The membranes were washed and incubated for 1 h with the primary anti-OLFM4 antibody (diluted 1:1000 in 5% skimmed milk powder in TBST). Then, the membranes were washed again and treated for 1 h with the secondary HRP-conjugated goat anti-mouse immunoglobulin G antibody (Immuno Research Laboratories, West Grove, PA, USA; diluted 1:5000 in 5% skimmed milk powder in TBST). Protein detection was performed using the Amersham™ ECL Plus Western Blotting Detection System (GE Healthcare, Chalfont St Giles, UK). Signals were visualized with a chemiluminescence camera charge-coupled device LAS-1000 (Fuji, Tokio, Japan). Densitometric analysis was performed with AIDA 2.1 software (Raytest, Straubenhardt, Germany).

After 24 h primary and secondary antibodies were removed from the membranes by incubation for 30 min in Restore™ Western Blot Stripping Buffer (Thermo Scientific, Rockford, IL, USA). Then, Dot Blot analysis was performed for ß-actin on the same membranes. The primary ß-actin antibody (Sigma, Deisenhofen, Germany) and also the secondary HRP-conjugated goat anti-mouse immunoglobulin G antibody (Immuno Research Laboratories, West Grove, PA, USA) were diluted 1:5000 in 5% skimmed milk powder in TBST. Detection of ß-actin was performed as described above. In sigma biopsies, OLFM4 protein content was

Table 1 Oligonucleotide primer pairs used for PCR measurements.

Product	Forward primer (5'- > 3')	Reverse primer (5'- > 3')
ß-actin	GCCAACCGCGAGAAGATGA	CATCACGATGCCAGTGGTA
IL-8	ATGACTTCCAAGCTGGCCGTGGC	TCTCAGCCCTCTTCAAAAACTTC
OLFM4	TGCCATTCGCCGAGAAATCGTGGCTCT	TCACCACACCACCATGACCACAGCTCC
Muc1	AGACGTCAGCGTGAGTGATG	CAGCTGCCCGTAGTTCTTTC
Muc2	ACCCGCACTATGTCACCTTC	GGGATCGCAGTGGTAGTTGT
Hath1	CGAGAGAGCATCCCGTCTAC	TCCGGGGAATGTAGCAAATA

normalized to ß-actin by dividing the densitometric intensity (LAU) of OLFM4 through the LAU of ß-actin in the same biopsy. Notably, OLFM4 and ß-actin, were exposed for the same time period (5 min).

2.7. HBD1-3/OLFM4 binding assay

To investigate the possibility that OLFM4 binds to the major colonic defensins, we developed an HBD1-3/OLFM4 binding assay. Therefore, 96 well plates (Nunc, Roskilde, Denmark) were coated for 3 times in triplicates overnight at 4 °C with 5 µg HBD1, HBD2 or HBD3 (Peptanova, Sandhausen, Germany) or 5 µg bovine serum albumin (BSA, Sigma, Deisenhofen, Germany) per well in 100 µl coating buffer (50 mM $NaHCO_3/Na_2CO_3$, pH 9.6). As a control, 100 µl coating buffer alone was used. The next day the wells were washed with TBST and blocked with 5% skimmed milk powder in TBST for 1 h. After repeatedly washing with TBST, the wells were incubated overnight at 4 °C with 0, 2 or 6 µg OLFM4 (Sino Biological, Beijing, China) in 100 µl 5% skimmed milk powder in TBST. Then, wells were washed again and incubated with the anti-OLFM4 antibody diluted 1:500 in 5% skimmed milk powder in TBST for 1 h. After repeatedly washing, wells were incubated with a HRP-labeled secondary antibody (Dako, Glostrup, Denmark) for 30 min. Again, wells were washed and thereafter incubated with 200 µl 2,2′-azino-bis-3-ethylbenzthiazoline-6-sulphonic acid (ABTS, Sigma, Deisenhofen, Germany) for 10 min. Photometric visualization was carried out with Wallac Victor™ 1420 Multilable Counter (Waltham, MA, USA) at 405 nm wave length.

2.8. Flow cytometric assay

Antimicrobial activity was measured with a flow cytometric test as described previously.[37] Briefly, suspensions of *Escherichia coli ATCC 25922* were grown overnight in Schaedler Broth (BD, Sparks, MD, USA) diluted 1:6 with sterile distilled water at 37 °C. Subsequently 1.5×10^6 mid-logarithmic-phase bacteria/ml in Schaedler Broth 1:6 in a final volume of 100 µl were incubated with 5 µg HBD1, HBD2 or HBD3 (Peptanova, Sandhausen, Germany) and 2 or 6 µg recombinant human OLFM4 (Sino Biological, Beijing, China) at 37 °C. Since OLFM4 is diluted 1 µg/µl in OLFM4-solvent buffer (0.2 µm filtered solution of PBS, pH 7.4, 3.2% glycerol, 8% trehalose, 8% mannitol) by the company, bacteria were also incubated with 5 µg HBD1-3 and 2 or 6 µl OLFM4 solution buffer alone (obtained by the company) for control experiments. Three independent experiments were performed in triplicates. After 90 min, 1 µg/ml of the membrane potential sensitive dye $DiBAC_4(3)$ (bis-(1,3-dibutylbarbituric acid) trimethine oxonol; Invitrogen, Carlsbad, CA, USA) was added. After 10 min of incubation, the samples were centrifuged for 10 min at 4500 g and the bacterial pellets were resuspended in 300 µl phosphate buffered saline (pH 7.4). With a FACSCalibur™ flow cytometer (BD, Sparks, MD, USA) 10000 events of each sample were analyzed for light scattering and green fluorescence. Antimicrobial activity was determined as percentage of fluorescent depolarized bacteria.

2.9. Cell culture experiments

The colon adenocarcinoma cell line LS174T (American Type Culture Collection, Manassas, USA) was cultivated in Dulbecco's modified Eagle medium (DMEM, Gibco Life Technologies, Eggenstein, Germany) completed with 10% fetal calf serum (FCS, PAA Laboratories, Pasching, Austria), 1% non essential amino acids (Gibco Life Technologies, Eggenstein, Germany), 1% penicillin/streptomycin (Gibco Life Technologies, Eggenstein, Germany) and 1% sodium pyruvate (Gibco Life Technologies, Eggenstein, Germany) in a humidified atmosphere at 37 °C and 5% CO_2. For experiments, cells were seeded for at least 3 times in triplicates into 12-well culture plates (Becton Dickinson, Franklin Lakes, New Jersey, USA) at a density of 0.65×10^6 per well. At about 70% confluence, cells were washed with phosphate-buffered saline (Gibco Life Technologies, Eggenstein, Germany) and incubated in FCS- and antibiotic-free DMEM for 12 h.

Then, cells were incubated with *E. coli K12*, *E. coli Nissle*, *Bacteroides vulgatus*, *Symbioflor G1/G2/G3*, *Lactobacillus fermentum* and *acidophilus*, as well as *Bifidobacterium longum*, *breve* and *adolescentis* for 6 and 24 h. All *E. coli* strains and *B. vulgatus* were cultivated under aerobic, *Lactobacilli* and *Bifidobacteria* under anaerobic conditions as previously described.[38] Bacteria were killed per heat inactivation in a water bath at 65 °C for 1 h. Then, bacteria were washed with PBS and adjusted to a density of 3×10^8 cells/ml with FCS- and antibiotic-free DMEM. To investigate the possible role of the Notch signaling pathway in regulating OLFM4, cells were incubated for 6 and 24 h with the γ-secretase inhibitor dibenzazepine (DBZ, Axon Medchem, Groningen, Netherlands) in a concentration of 1 µM (in 0.1% DMSO in DMEM) in the absence or presence of *E. coli Nissle*. LS174T cells were also treated with 10 ng/ml TNF-α (Sigma, Deisenhofen, Germany), 100 ng/ml IL-22 (Sigma, Deisenhofen, Germany), 10 ng/ml IL-4 (Sigma, Deisenhofen, Germany) and 10 ng/ml IL-13 (Sigma, Deisenhofen, Germany) for 6, 12 and 24 h. At the end of experiments cells were washed with PBS and mRNA was isolated using RNeasy Mini Kit (Qiagen, Venlo, Netherlands) according to the supplier's protocol.

2.10. Statistics

Statistical analyses were performed and all graphs were generated with the GraphPad Prism version 4.0 software using the Mann–Whitney test. In case of the PCR measurements in human sigma biopsies, Bonferroni correction was also done. Spearman's rank analysis was performed for nonparametric correlation between the different subgroups of the quantitative real-time PCR results. Values of $p<0.05$ were considered to be statistically significant. Data are presented in box and whiskers (means).

3. Results

3.1. OLFM4 and mucins are differentially expressed in inflamed IBD

In colonic biopsies transcripts of the proinflammatory cytokine IL-8 (Fig. 1A) were equally enhanced in inflamed CD

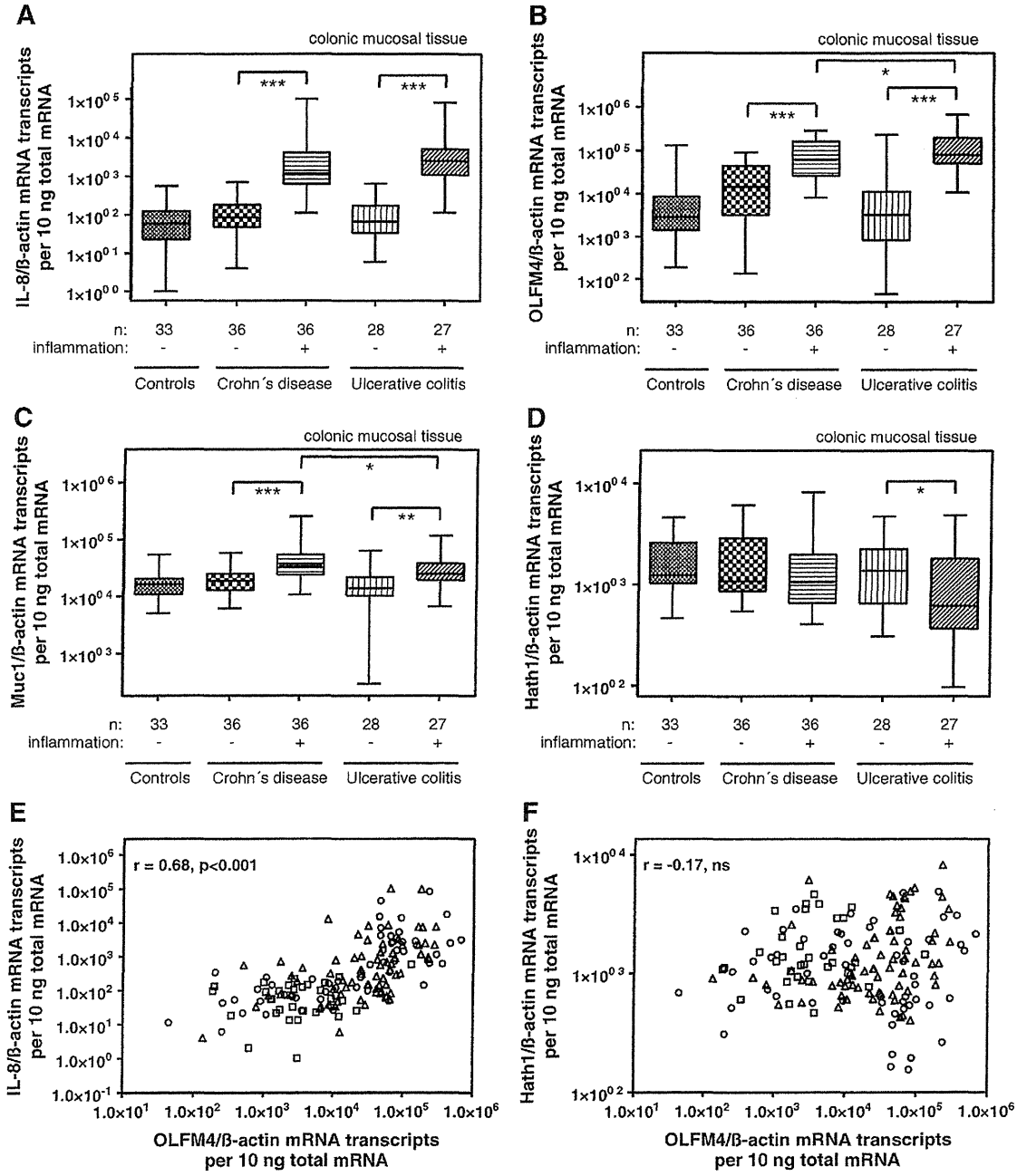

Figure 1 IL-8, OLFM4, Muc1 and Hath1 expression in controls and IBD mucosa: IL-8 transcripts are enhanced in inflamed vs. noninflamed CD and UC without significant differences between both diseases (A). OLFM4 mRNA was significantly more induced in UC than CD (B). Muc1 transcripts are augmented more in inflamed vs. noninflamed CD than in UC (C). Hath1 mRNA is significantly downregulated in inflamed UC (D). OLFM4 is highly correlated with IL-8 (E, $r=0.68$ for all samples, $p<0.001$) but not with Hath1 (F, $r=-0.17$ for all samples, ns; squares = controls, triangles = CD, circles = UC; *: $p<0.05$ (these significances are lost after Bonferroni correction), **: $p<0.01$, ***: $p<0.001$).

(14-fold, $p<0.001$) and UC (38-fold, $p<0.001$) compared to the respective noninflamed samples. In controls and noninflamed IBD samples IL-8 expression was comparably low. The grade of histological inflammation was similar in both inflamed IBD entities (inflammation score for controls: 1.0, for CD: 7.2 and for UC: 7.0). The CAI was 2.6 for the noninflamed UC group and 12.1 for the inflamed UC patients. The CDAI was 188 in case of noninflamed colonic CD and 237 in inflamed colonic CD patients.

OLFM4 mRNA (Fig. 1B) was significantly induced in inflamed CD (4.3-fold, $p<0.001$) and UC (24.8-fold, $p<0.001$) vs. noninflamed biopsies. This upregulation was clearly

higher in inflamed UC than in inflamed CD samples (5.8-fold, p=0.04). Again, controls and noninflamed samples were in the same range. Immunostaining for OLFM4 in normal human colonic tissues was confined to the lower third of crypts but expanded during inflammation up to the epithelial surface (Fig. 2). The OLFM4 protein content normalized to ß-actin as determined by Dot Blot analysis (Fig. 3) was also clearly augmented in inflamed CD (1.7-fold, p=0.03) and UC (3.7-fold, p=0.03) as compared to controls. Again, this induction was numerically more pronounced in inflamed UC as compared to inflamed CD (ns).

Muc1 transcripts (Fig. 1C) were also significantly augmented in inflamed CD (1.9-fold, p<0.001) and UC (1.8-fold, p=0.002) samples as compared to controls. In contrast to OLFM4, this induction was less significant in inflamed UC

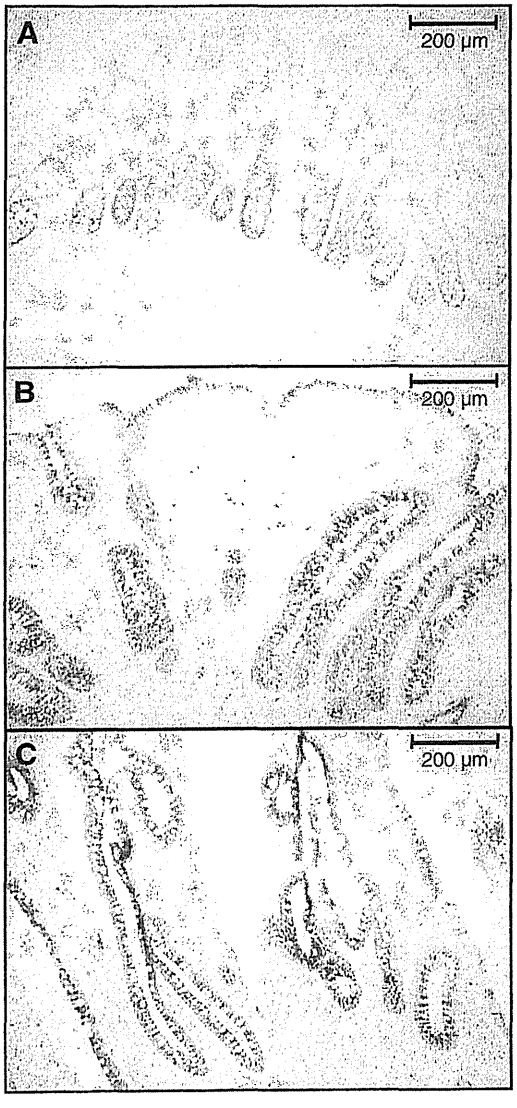

Figure 2 OLFM4 immunostaining in controls and IBD mucosa: OLFM4 staining is located in the lower third of the crypt in control samples (A, magnification 100-fold) and expanded up to the epithelial surface during inflammation (B = inflamed CD, C = inflamed UC, magnification 100-fold).

than in inflamed CD biopsies (p=0.03). Controls and noninflamed samples exhibited a comparable expression. Muc2 mRNA levels did not show significant differences between the 5 subgroups (data not shown). Hath1 expression (Fig. 1D) was significantly lower in inflamed vs. noninflamed UC (0.7-fold, p=0.02) but not CD. Transcripts of OLFM4 correlated significantly with IL-8 (Spearman r: 0.68, p<0.001, Fig. 1E) and Muc1 (r: 0.57, p<0.001) but not with Hath1 (r: −0.17, ns, Fig. 1F).

3.2. OLFM4 is secreted into the mucus and binds to ß-defensins HBD1-3

Since OLFM4 is upregulated in inflamed IBD and staining was found up to the epithelial surface, we searched for OLFM4 protein in human mucus following Carnoy-fixation. Indeed, rectal IBD biopsies showed a positive immunostaining for OLFM4 in the crypt lumen (Fig. 4A) as well as in the surface mucus (Fig. 4B), implying the secretion of OLFM4 by epithelial cells into the mucus. This observation was confirmed in rectal mucus extracts, which were obtained by colonoscopic brushings and analyzed with the Dot Blot technique (Fig. 4C): OLFM4 protein was found in the mucus of patients with inflamed CD and even more pronounced in patients with inflamed UC, whereas noninflamed mucus controls were almost negative. As expected, ß-actin was only marginally detectable in mucus showing that these extracts were almost free of cell detritus.

The defensins HBD1-3 are positively charged and also secreted into the mucus[10] whereas OLFM4 has a negative charge. Therefore, we tested the ability of recombinant OLFM4 to bind HBD1-3 preabsorbed to plastic wells. In contrast to no binding to BSA, OLFM4 preferentially bound to preabsorbed HBD3>HBD2 and >HBD1 (Fig. 5). Next, we checked the antimicrobial activity of HBD1-3 in the absence and presence of OLFM4. The coincubation of defensins with OLFM4 at 2 and 6 µg/ml was associated with a limited reduction of the antimicrobial activity in case of HBD1 from 66% to 58% (2 µg/ml, ns) and 47% to 39% (6 µg/ml, ns), in case of HBD2 from 69% to 54% (2 µg/ml, ns) and from 57% to 41% (6 µg/ml, ns) and in case of HBD3 from 71% to 65% (2 µg/ml, ns) and from 55% to 51% (6 µg/ml, ns).

3.3. Bacteria and IL-22 induce OLFM4 expression in LS174T cells

The mucin producing colon adenocarcinoma cell line LS174T was incubated with heat killed *E. coli K12*, *E. coli Nissle*, *B. vulgatus*, *Symbioflor G1/G2/G3*, *L. fermentum* and *acidophilus*, as well as *B. longum*, *breve* and *adolescentis*. An incubation for 24 h with *E. coli K12* (2.8-fold induction, p=0.009), *E. coli Nissle* (2.5-fold, p=0.02) and *B. vulgatus* (1.9-fold, p=0.02) led to a significant increase of OLFM4 expression in these LS174T cells. In contrast, OLFM4 was unaffected by heat killed *Symbioflor G1/G2/G3*, *L. fermentum* and *acidophilus*, as well as *B. longum*, *breve* and *adolescentis* (data not shown).

In addition, LS174T cells showed a significant time-dependent increase of OLFM4 expression following a treatment with 100 ng/ml IL-22 (3.4-fold after 6 h, p=0.04; 5.3-fold after 12 h, p=0.01; 9.1-fold after 24 h, p=0.01). In